Current Research in Structural Biology 4 (2022) 285–307

Contents lists available at ScienceDirect

Current Research in Structural Biology

journal homepage: www.journals.elsevier.com/current-research-in-structural-biology

Protein conformation and biomolecular condensates

Diego S. Vazquez, Pamela L. Toledo, Alejo R. Gianotti, Mario R. Ermácora *

Departamento de Ciencia y Tecnología, Universidad Nacional de Quilmes and Grupo de Biología Estructural y Biotecnología, IMBICE, CONICET, Universidad Nacional de Quilmes, Argentina

ARTICLE INFO

Handling editor: Dr G Rudenko

Keywords:
Phase separation
Intrinsically disordered proteins
Protein condensates
Protein conformation
Protein folding
Membraneless organelles
Mesoscopic clusters
Nanocondensates
Protein coacervates
Protein colloids

ABSTRACT

Protein conformation and cell compartmentalization are fundamental concepts and subjects of vast scientific endeavors. In the last two decades, we have witnessed exciting advances that unveiled the conjunction of these concepts. An avalanche of studies highlighted the central role of biomolecular condensates in membraneless subcellular compartmentalization that permits the spatiotemporal organization and regulation of myriads of simultaneous biochemical reactions and macromolecular interactions. These studies have also shown that biomolecular condensation, driven by multivalent intermolecular interactions, is mediated by order-disorder transitions of protein conformation and by protein domain architecture. Conceptually, protein condensation is a distinct level in protein conformational landscape in which collective folding of large collections of molecules takes place. Biomolecular condensates arise by the physical process of phase separation and comprise a variety of bodies ranging from membraneless organelles to liquid condensates to solid-like conglomerates, spanning lengths from mesoscopic clusters (nanometers) to micrometer-sized objects. In this review, we summarize and discuss recent work on the assembly, composition, conformation, material properties, thermodynamics, regulation, and functions of these bodies. We also review the conceptual framework for future studies on the conformational dynamics of condensed proteins in the regulation of cellular processes.

1. Introduction

Protein conformation results from a complex interplay of physicochemical forces acting on protein and solvent atoms. At molecular level, these forces cause rotation about *n* backbone and side-chains bonds, optimizing atom-atom interactions and leading ultimately to energy minima in an *n*-dimensional conformational space. At the whole system level, solvent and protein atoms interact, both intramolecularly and intermolecularly, shaping the conformational space (Nassar et al., 2021).

At different energy minima, protein conformation exhibits distinct order and compaction. Historically, its study began with proteinaceous materials in the form of multi-chain insoluble fibers, a highly compact and ordered state, likely at the lowest energy minimum of the conformational space (Astbury and Street, 1931). With the advent of the X-ray crystallography of soluble proteins (Bernal and Crowfoot, 1934), the attention turned to the native, biologically active conformation, which given its crucial role in the living matter became synonymous with protein structure and overshaded other possible conformational states.

After the recognition of the native state as the conformation of the biologically active protein, the unfolded state was conceived as an ideal reference state. In the ideal unfolded state there are at any instant as many conformations as protein molecules, random conformations fluctuate freely, and solvent–protein interactions, protein–protein and solvent–solvent interactions are as likely. No real protein can exist in the ideal unfolded state because there is not a real solvent able to interact equally well with all different protein residues and with itself. However, strongly concentrated solutions of chemical denaturants, such as urea and guanidinium chloride, mimic the ideal solvent, unfolding and separating protein chains, and thus providing an useful experimental model for the unfolded state (Peran et al., 2019).

Ensuing studies of protein conformation unveiled the existence of states that were neither native nor unfolded. These heterogeneous states have been termed 'partially folded' or 'molten globule' states. At first, to qualify as a partially folded state, it sufficed to exhibit complete loss of tertiary structure in a context of high compactness. With time, striking differences were observed between partially folded states with different degree of compaction, secondary structure content, and solvation (Uversky and Finkelstein, 2019).

For many decades, partially folded states were regarded as either productive intermediates or dead ends in the folding pathway. Moreover, their strong tendency to associate, aggregate and precipitate was

* Corresponding author. Departamento de Ciencia y Tecnología, Universidad Nacional de Quilmes, Roque Sáenz Peña 325, 1876, Bernal, Buenos Aires, Argentina.
E-mail address: ermacora@unq.edu.ar (M.R. Ermácora).

https://doi.org/10.1016/j.crstbi.2022.09.004
Received 4 August 2022; Received in revised form 8 September 2022; Accepted 13 September 2022

Abbreviations

ALS	amyotrophic lateral sclerosis
CLD	cross linking domain
DLS	dynamic light scattering
ELP	elastin like polypeptide
ETM	electronic transmission microscopy
FTD	frontotemporal dementia
HD	hydrophobic domain
IDR	intrinsically disordered region
IDD	intrinsically disordered domain
IDP	intrinsically disordered protein
LCD	low complexity domain
LLPS	liquid–liquid phase separation
LSPS	liquid–solid phase separation
MLO	membraneless organelle
OIM	oblique illumination microscopy
PLD	prion like domain
PQC	protein quality control
RBD	RNA binding domain
RBP	RNA binding protein
RRM	RNA recognition motif
SLS	static light scattering
SG	stress granule

considered an *in vitro* nuisance rather than a biologically relevant feature. Only recently, the widespread physiological and pathological existence of partially folded states has come into recognition. Initially, these proteins have been loosely termed 'natively unfolded' proteins, which is misleading. In fact they are not unfolded, but they are partially folded states that may or may not acquire a structured native state under certain conditions.

The term 'natively unfolded' has been progressively replaced by 'intrinsically disordered', which is still uninformative of the real conformational state, but at least it does not misrepresent its nature. More importantly, the scope of the name was greatly expanded by the realization that in all kingdoms of life there are numerous intrinsically disordered proteins (IDPs) and also folded proteins with intrinsically disordered regions (IDRs). The latter is clearly illustrated by the fact that more than 70% of signaling proteins possess long IDRs (Uversky and Dunker, 2010; Mittal et al., 2018; Chong and Mir, 2021).

In its time, the concept that native domains and disordered regions could coexist in a biologically active protein was highly disruptive because (a) folding had been always regarded as a cooperative, all-or-none process in which all parts of the protein chain contribute to the marginal stability of the folded molecule, and (b) unfolded structures had been customarily considered devoid of function. However, the modern concept of domain as the unit of protein structure reconciles order, disorder and biological function. In fact, if one defines IDRs as rightly domains and thinks of multidomain proteins as composed of coexisting folded and intrinsically disordered domains (IDDs), a general function for the latter is envisaged: to allow multiple, long-range, and fuzzy interactions with different ligands and partners in large biological complexes (Tompa and Fuxreiter, 2008); Uversky and Dunker (2010); Van Der Lee et al., 2014; Uversky and Finkelstein (2019); Mohanty et al. (2022).

In the last decades, we have witnessed exciting advances that unveiled the strong connection between conformational disorder and the phase separation phenomenon of protein biomolecular condensation, a phase separation phenomenon that causes a membraneless compartmentalization of cells. An avalanche of observations and experiments highlighted the central role of biomolecular condensates —such as liquid-like membraneless organelles (MLOs) and solid-like protein condensates— in subcellular compartmentalization (Banani et al., 2017). In most cases, the main driving force for the formation of biomolecular condensates is intermolecular affinity of IDDs (Hyman et al., 2014).

The realization that IDDs are strongly involved in phase separation is of paramount importance. Indeed, it establishes a link between conformational change at molecular level and a mesoscopic property. Conceptually, this link also inaugurates a higher dimension in the protein folding theory, by which protein condensation can be thought of as folding of large assemblies of protein molecules. In this expanded view, intramolecular folding is a single-chain disorder-to-order transition, and intermolecular folding is a multi-chain disorder-to-order transition (Miskei et al., 2020; Nassar et al., 2021). In dilute solutions of individually folded proteins, main interactions are intramolecular and lead to well-defined equilibrium structures. In condensed phases, protein concentration is much higher and protein–protein interactions prevail, leading to dynamic networks of interacting molecules lacking fixed stoichiometry and structural uniqueness. The concept of quinary structure was developed to capture this supramolecular hierarchical level of protein organization (Guin and Gruebele, 2019).

Many MLOs properties can be mimicked by condensates formed *in vitro* through liquid–liquid phase separation (LLPS) of protein constructs (P. Li et al., 2012). Moreover, expression *in vivo* of such constructs leads to LLPS, which firmly establishes the connection between colloid chemistry and biomolecular condensation (Nott et al., 2015; Shin and Brangwynne, 2017; Yewdall et al., 2021). In turn, solid-like protein condensates, a heterogeneous collection of bodies and proteinaceous materials, can emerge from metastable liquid condensates through liquid–solid phase separations (LSPS).

Protein conformation in the condensed state is the subject of this review. However, given its vastness, we mostly focus on the protein conformation in liquid condensates. Several excellent and recent reviews on the multiple aspects of protein condensation are available, and the interested reader is directed to them for more information on specialized aspects of the subject (Uversky, 2017; Banani et al., 2017; Holehouse and Pappu, 2018a; Peran and Mittag, 2020; Choi et al., 2020; Alberti and Hyman, 2021; Lyon et al., 2021; Abyzov et al., 2022; Mohanty et al., 2022). In this review, we endeavored to cover the subject from a structural biology perspective and to exhaustively illustrate with examples the ideas and basic principles discussed.

2. Biological relevance of phase separation

In biology, phase separation is a physical process that originates a macromolecular, condensed phase immersed in a macromolecular dilute phase. It is a self-organizing process that results in compartmentalization and concentration of biomolecules involving neither membrane enclosure nor cumbersome transport mechanisms. In turn, compartmentalization permits the spatiotemporal organization and regulation of myriads of simultaneous biochemical reactions and macromolecular interactions (Hyman et al., 2014; Shin and Brangwynne, 2017; Holehouse and Pappu, 2018a; Mathieu et al., 2020; Lyon et al., 2021). A model was recently proposed that considers three interconnected levels of spatial organization in cellular condensation. 1D organization allows alignment of condensates along locally linear structures, such as DNA, microtubules, or the cytoskeleton. Phase separation on and within membranes, 2D organization, permits condensates to adhere to surfaces and physically connect different cellular compartments. 3D organization efficiently pervades large volumes independently of external scaffolding structures. These three levels influence each other and work in concert to adjust cell signaling and metabolic systems to changing demands (Nesterov et al., 2021). Based on sequence similarity, it has been speculated that as much as 20% of the proteome participates in LLPS (Vernon and Forman-Kay,

2019; Hardenberg et al., 2020).

Biologically relevant condensed phases encompass a variety of materials: liquid-like, gels, solid-like aggregates, fibers, amyloids, and ordered quasi-crystal solids. There is an emerging consensus that many of the different condensates arise from initial LLPS, which provides the necessary high concentration of the involved biomolecules. Frequently, condensed phases are further structured in subphases. The use of the term phase here does not necessarily imply physicochemical equilibrium. On the contrary, condensed phases frequently are highly dynamic and far from equilibrium. Although all kind of biomolecules may participate, proteins and nucleic acids are the major players in biomolecular condensation (P. Li et al., 2012).

As an emerging paradigm of cellular organization, phase separation has been associated with most important biological processes in all forms of life. Indeed, phase separation of macromolecules may be traced back to the origin of life (Keating, 2012; Hyman et al., 2014; Yoshizawa et al., 2020; Ghosh et al., 2021).

A number of reviews have appraised the emergence of phase separation as a new mesoscale organizational principle in cell biology, akin to compartmentalization by membranes (see for instance Holehouse and Pappu, 2018b; Turoverov et al., 2019; Lyon et al., 2021; Feng et al., 2021). Thus, an exhaustive review of this principle is beyond of the scope of this work, and only a selection of paradigmatic examples of the biological relevance of membraneless phase separation will be presented.

2.1. Nuclear pore complex

Exchange of macromolecules between the nucleus and the cytoplasm is achieved through nuclear pore complexes (NPCs). NPCs are extremely large molecular assemblies of over 100 MDa, involving multiple copies of over 30 different proteins termed nucleoporins (Nups). They comprise a scaffold for anchoring to the nuclear envelope and a central aqueous channel. Through the channel, mature RNA species, ribonucleoproteins, and ribosomal subunits are exported to the cytoplasm, and nuclear proteins are imported into the nucleus (Frey and Görlich, 2007; Schmidt and Görlich, 2016).

Many Nups contain IDDs that are rich in FG repeats and allow the assembly of a physical barrier embedded in the NPCs. This barrier is freely permeable to small molecules but selective to large macromolecules and ribosomal particles. This remarkable property stems from its constitution by phase separation into a dense liquid-condensate, akin to a hydrogel (Celetti et al., 2020).

The hydrogel properties and multivalency of Nups FG repeats allow two translocation modes: passive diffusion mediated by size exclusion and facilitated translocation mediated by the affinity for FG domains of nuclear transport receptors (NTRs). The translocation interactions are typically of very weak affinity and high valency, and the selectivity of these sieve-like barriers is endowed by the ability to interact with appropriate shuttling NTRs, which bind to Nups FG motifs as well as to their specific cargoes (Schmidt and Görlich, 2016).

2.2. RNA-protein condensates

A large number of cell bodies are formed by condensation of RNA-binding proteins (RBPs) and RNA, a condensation that is promoted by the polyanionic, multivalent nature of RNA. RBPs exhibit broad specificity and affinity for RNA (Kiledjian and Dreyfuss, 1992). Typically, they comprise RNA binding domains (RBDs) and low-complexity domains (LCDs). LCDs show enrichment of certain residue types or sequence repeats. Some LCDs also exhibit sequence features of prion-like domains (PLDs) (Molliex et al., 2015; Patel et al., 2015; Wang et al., 2018; Martin and Mittag, 2018). Strikingly, a significant proportion of RBPs with PLDs have been implicated in the pathology and genetics of devastating degenerative disorders (King et al., 2012). Prominent examples of ribonucleoprotein condensates are: nucleoli, *P* granules, stress granules, germ granules, Cajal bodies, Balbiani bodies, nuclear *A* bodies, paraspeckles, and bacterial ribonucleoprotein bodies (BR-bodies) (Banani et al., 2017; Yoshizawa et al., 2020; Roden and Gladfelter, 2021).

Nucleoli are essential RNA–protein condensates involved in the biogenesis of ribosomes, the regulation of the cell-cycle, and in the response to stress. The assembly of ribosomes is a very complex process involving several hundred of components and factors. Different phase-separated nucleolar subcompartments partake in the synthesis and assembly of ribosomal particles: the fibrillar center (FC), the dense fibrillar component (DFC), and the granular component (GC). rDNA gene arrays are anchored in the FC. Transcription of rDNA takes place at the FC/DFC interface. In the DFC compartment, nascent pre-rRNA transcripts undergo processing, modification, and folding. The assembly of pre-ribosomal particles occurs in the GC nucleolar component. Additional assembly, remodeling and processing take place in the nucleoplasm before export to the cytoplasm. Specific RNAs and intrinsically disordered, multivalent protein domains contribute to the LLPS and material characteristics of each nucleolar subcompartment (Boisvert et al., 2007; Correll et al., 2019; Latonen, 2019; Sawyer et al., 2019).

P granules are ribonucleoprotein condensates found in the cytoplasm of *C. elegans* embryos that store maternal factors and participate in the specification of germ-cells. Similar condensates are found in germ cells of various metazoans, including mammals. *P* granules are involved in the regulation of development, as they dissolve at the anterior end of the posterior–anterior axis and condense at the posterior end (Brangwynne et al., 2009). Interestingly, some of the RBPs in the *P* granules contain FG-rich IDDs. This strongly suggests that the cohesive interactions between their components are similar to those seen in the NPCs hydrogels. In contrast to NPCs hydrogels, *P* granules fuse and deform in response to flow; like NPCs hydrogels, *P* granules may act as molecular sieves and extend the NPCs mesh (Updike et al., 2011).

Cajal bodies (CB) and the histone locus bodies (HLB) are nuclear bodies with distinct functions in ribosome biogenesis, spliceosomal small nuclear ribonucleoprotein assembly, telomere maintenance, and histone mRNA 3' end formation. CBs and HLBs harbor dozens of proteins and RNA components. Interactions between IDDs of RNA-binding proteins and different RNAs cause phase separation into the hydrogel-like state of these nuclear bodies (Machyna et al., 2013).

Stress granules (SGs) are cytosolic granules formed by RBPs and mRNA whenever translation initiation is inhibited by drugs or by stress responses (Protter and Parker, 2016). SGs are enriched in RBPs proteins that *per se* phase separate *in vitro* (Molliex et al., 2015). These SGs proteins contain intrinsically IDDs and interact multivalently with each other and with RNA. In addition to the RBPs, SGs contain many other non-RNA binding proteins recruited by protein-protein interactions, including post-translation modification enzymes, metabolic enzymes, and protein or RNA remodeling complexes. Importantly, the protein composition of SG varies under different conditions (Protter and Parker, 2016). SGs contain stable core substructures, which implies that liquid condensation may be an initial step in the formation of more complex, condensed states. *In vitro* experiments suggest that amyloid-like substructures in the SGs may be behind a maturation process of protein chains with PLDs, which in certain circumstances can even originate pathological fibrillar deposits. In this regard, several degenerative diseases are caused by pathological fibrillation of SGs proteins (Patel et al., 2015; Molliex et al., 2015; Protter and Parker, 2016; Youn et al., 2019).

Balbiani bodies are constituted by RNA, proteins, and organelles such as mitochondria, endoplasmic reticulum, and Golgi stacks. They can be found in dormant, non-growing oocytes and disassemble during oocyte maturation. It is believed that Balbiani bodies keep the organelles in a low-activity, dormant state for decades until the oocyte receives maturation signals (Woodruff et al., 2018). The Balbiani body matrix is formed by the protein Velo1, which is highly concentrated and constitutes a scaffold that keep the organelles together. Velo1 contains IDDs and a PLD. As just mentioned, PLDs are known to promote the formation of liquid-like condensates with the capacity to evolve into solid amyloid-like aggregates (Roden and Gladfelter, 2021).

A bodies, like the Balbiani bodies, are reversible nuclear *foci* that score positive for the amyloid-specific dyes thioflavin S and Congo red. The *A* bodies are primed by a long non-coding RNA, rlGSRNA, and congregate cyclin-dependent kinases, histone deacetylases, and ubiquitin ligases, leading to cell-cycle arrest (Woodruff et al., 2018).

Paraspeckles, transcription-related condensates in interphase nuclei, are scaffolded by the long, non-coding RNA NEAT1. Over 40 different, mostly ubiquitous, RNA binding proteins are associated to paraspeckles. Most of the paraspeckle proteins contain PLDs, hinting that physiological amyloidogenesis may be involved in their formation (Fox et al., 2018).

BR-bodies are condensates of the RNA degradosome that selectively sequester mRNA for degradation. These condensates are scaffolded by the C-terminal domain of RNase E, which is an IDD and contains many RNA-binding sites. BR-bodies are modulated by translation and their disassembly is promoted by mRNA cleavage (Azaldegui et al., 2021).

2.3. Centrosomes

The centrosomes are membraneless organelles involved in the assembly of the mitotic spindle. They comprise a pair of centrioles immersed in a pericentriolar material that expands greatly during mitosis. Upon phosphorilation, specific coiled-coil proteins make a scaffold for the mitotic pericentriolar condensate and recruit tubulin, kinases, and other proteins that promote microtubule formation through the nucleation and polymerization of soluble α/β tubulin dimers.

The mitotic-spindle microtubules nucleated within the centrosomes form the spindle apparatus. At the end of mitosis, the mitotic pericentriolar condensate disassembles. *In vitro* assembling experiments and live-cell observations suggest that the pericentriolar material begins as a dynamic liquid-like condensate an matures into a porous gel-like material (Woodruff et al., 2018). During mitosis, sister chromatids are positioned on the spindle midplane to drive chromosomes segregation into daughter cells. The spindle apparatus is a complex array of dynamic microtubules embedded in the spindle matrix, a meshwork formed by LLPS (Tiwary and Zheng, 2019).

2.4. Membrane-associated condensates

Liquid phases juxtaposed to lipid membranes can induce the formation of membrane-associated protein condensates (Zhao and Zhang, 2020; Ditlev, 2021; Botterbusch and Baumgart, 2021; Wu et al., 2022). Several of them have been characterized experimentally: T-cell condensates of LAT and its binding partners; the podocyte filtration-barrier protein nephrin; postsynaptic density proteins PSD-95, Homer3, Shank3, and DLGAP; tight junction protein ZO-1; and cell polarity proteins Par3/Par6/aPKC and Numb/Pon. Other membrane-associated clusters of proteins that are presumed to phase-separate are focal adhesions, growth-factor receptor clusters, chimeric antigen-receptor clusters, organelle–organelle tethers or contacts, and Golgi complexes.

2.5. Condensates in metabolism control, signaling, cell adhesion, and protein trafficking

By facilitating segregation, proper localization, and concentration of interacting macromolecules, phase separation is involved in the spatio-temporal control of cellular processes. In the absence of limiting membranes, affinity-controlled diffusivity allows rapid changes in the composition of biomolecular condensates and rapid disassembly in response to signaling events. Both affinity and composition are sensitive to environmental changes, such as concentration, pH, and ionic strength. In addition, protein posttranslational modifications —including phosphorylation, methylation, ubiquitination, and sumoylation— modulate the biophysical and biochemical properties of the condensates. This broad sensitivity to multiple factors endows condensates with the capacity of integrating a variety of signals.

An example of metabolism control by condensates is that of the cyanobacterium *S. elongatus*, in which at night multiple metabolic enzymes form *puncta* that dissolve during the day. Accordingly, mutations that disrupts the day-night cycle of gene expression and cell division alter *puncta* formation, and thus reversible condensation of specific enzymes may adjust to the circadian clock (Pattanayak et al., 2020).

Signaling is a biochemical process carried out by multicomponent protein complexes. These complexes have been envisaged as precisely-defined, stoichiometric interactions between proteins. However, recently it took shape the concept of signaling through non-stoichiometric, fuzzy assemblies in condensates. These signaling condensates may be tied to membranes trough membrane-bound components, connecting cellular and extracellular compartments. This liaison between organelles and condensates may be the driving force behind receptor clustering, a general mechanism in signaling (Banjade and Rosen, 2014; Snead and Gladfelter, 2019).

Wnt signaling plays a key role in the transformation of fertilized eggs into the different animal body cells and in cell fate through tissue homeostasis. Wnt ligands belong to a large family of secreted growth stimulatory factors that signal through the transmembrane Frizzled (Fz) receptor. The Wnt receptor complex includes: Wnt, Fz, low-density lipoprotein receptor-related protein 5 and 6, and Dishevelled. This complex recruits the inactive destruction complex (Axin, Ser/Thr kinases GSK-3 and CK1, and tumor suppressor APC) and causes a rise in cytoplasmic β-catenin. In turn, entering the nucleus, β-catenin binds to the TCF/LEF family of transcription factors and co-activates transcription of Wnt target genes. In the absence of Wnt, the destruction complex is activated by binding and phosphorylating β-catenin, which is targeted to the proteasome and destroyed via β-TrCP–E3-ubiquitin ligase (Chong and Forman-Kay, 2016; Nusse and Clevers, 2017; Schaefer and Peifer, 2019).

Two key components of the Wnt destruction complex, APC and Axin, are multivalent scaffolding proteins containing folded and intrinsically disordered domains that bind β-catenin and other proteins. Axin forms large *puncta* that recruits APC and other destruction complex proteins. APC is required for *puncta* assembly *in vivo*, and *puncta* localization is regulated by Wnt signaling. Accumulating evidence suggests that the destruction complex is a biomolecular condensate with a structured scaffold built around intertwined Axin and APC polymers (see Schaefer and Peifer, 2019, and references therein).

The nephrin adhesion complex and TCR signaling cluster are two examples of clusters formed by phase separation close to the plasma membrane. Both are triggered by multivalent binding of SH3 and SH2 domains to phosphorylated tyrosine- and proline-rich motifs (Zhao and Zhang, 2020). Nephrin ectodomain participates in the formation of zipper-like intercellular junctions and transduces a phosphotyrosine signal through several phosphorylation sites in its cytoplasmic domain. Nephrin, N-Wiskott-Aldrich syndrome protein (N-WASP), and the non-catalytic region of tyrosine kinase (NCK) phase-separate through multivalent interactions. In turn, the condensate recruits and activates the Actin Related Protein 2/3 complex —a seven-subunit protein complex that plays a major role regulating the actin cytoskeleton—, which triggers actin polymerization (Banjade and Rosen, 2014; Chong and Forman-Kay, 2016; Zhao and Zhang, 2020).

T-cells and antigen-presenting cells interact through the T-cell receptor (TCR) and the antigen-occupied major histocompatibility complex (MHC) in the respective cell membranes. As a result, T lymphocytes are activated through signal transduction. Lymphocyte-specific protein tyrosine kinase (LCK) phosphorylates the cytoplasmic domain of the TCR, and TCR phosphorylation is reversed by CD45, a transmembrane phosphatase. TCR phosphorilation recruits and activates cytosolic tyrosine kinase ZAP70. In turn, ZAP70 phosphorylates multiple tyrosine residues of the transmembrane protein linker for activation of T cells (LAT), which engages the SH2 and SH3 domain-containing protein GRB2 and SOS1 for activation of mitogen-activated protein kinase (MAPK) signaling. Phosphorylated LAT elicits phase separation with GRB2 and SOS1 (Su et al., 2016; Lin et al., 2022).

Some other selected examples of signaling condensates are the following: the membrane-bound condensate formed by Numb and its adaptor Pon during the neuroblast asymmetric cell-division that initiates differentiation in *Drosophila* (Zhao and Zhang, 2020); the clustering of cystic fibrosis transmembrane conductance regulator (Chong and Forman-Kay, 2016); the signaling inflammasome, necrosome, and signalosome (Parry et al., 2015); the synapsin condensate that captures and accumulates synaptic vesicles at nerve terminals (Milovanovic et al., 2018); and the phase separation that regulate protein organization at presynaptic membranes (Milovanovic et al., 2018).

Tight junctions are selective diffusion barriers between cells. In tight junctions, transmembrane adhesion proteins, such as occludins and claudins, are connected to cytoplasmic scaffolding zona occludens proteins (ZO) and to cingulins. ZO proteins form a membrane-associated scaffold through multivalent interactions of PDZ-SH3-GuK domains which recruits cytoskeleton and signaling proteins. Phase separation of ZO proteins is inhibited by phosphorylation, and dephosphorylation of ZO triggers spatially controlled assembly of ZO condensates (Zihni et al., 2016; Beutel et al., 2019; Schwayer et al., 2019; Rouaud et al., 2020).

Secretory granules are membrane-limited organelles formed in the Golgi complex and transported to the plasma membrane for regulate secretion. Within secretory granules, hormones are stored as condensates with properties ranging from liquids to semi crystalline solids, and which dissolve upon secretion (Dodson and Steiner, 1998; Maji et al., 2009; Kienzle and von Blume, 2014). These condensates could be isolated free of membranes by mild detergent treatment and sedimentation (Giannattasio et al., 1975; Michael et al., 1987), which confirms their entity as separated phases. Recently, liquid chromogranin condensates were found involved in recruiting and sorting of proinsulin and other granule-destined cargo molecules (Parchure et al., 2021).

2.6. Pathological condensates

Protein condensates have been linked to the formation of pathological amyloid-like aggregates in an impressive number of diseases: amyotrophic lateral sclerosis (ALS), frontotemporal dementia (FTD), Alzheimer, Huntington, Parkinson, Creutzfeldt-Jakob, Kuru, familial insomnia, transthyretin familial amyloid polyneuropathy, type II diabetes, multiple myeloma, cystic fibrosis, neurohypophyseal diabetes insipidus, nephrogenic diabetes insipidus, spinocerebellar ataxia, Fabry, spinal bulbar muscular atrophy, sickle cell anemia, retinitis pigmentosa, Niemann-Pick, Gaucher, myofibrillar myopathies, and others (Yadav et al., 2019).

The amyloid-like, fibrillar aggregates were once assumed to be the cause of conformational diseases; now, their are increasingly seen as late manifestations of a more general disorder (Mathieu et al., 2020). Protein homeostasis (proteostasis) involves control of protein synthesis, folding, and degradation, and therefore it is directly implicated in the formation of protein condensates. Disruption of proteostasis underlies the formation of most pathological condensates. In this regard, although protein mutations or deletions are major factors, environmental stress and aging also contribute to pathology, since numerous proteins are aggregation prone in these conditions (Kundra et al., 2017; Boeynaems et al., 2018; Klaips et al., 2018; Aarum et al., 2020).

ALS is a paradigmatic protein conformational disease characterized by the progressive degeneration of motor neurons and paralysis (Lagier-Tourenne et al., 2010) The hallmark of ALS is the deposition within motor neurons and surrounding glia of TAR DNA-binding protein 43 (TDP-43), superoxide dismutase-1 (SOD1), or the protein fused in sarcoma (FUS). Suggestively, TDP-43, SOD1, and FUS are capable of forming amyloid fibrils *in vitro*, and accumulating evidence suggests that SOD1 and TDP-43 do the same *in vivo* (McAlary et al., 2020).

Another disease characterized by phase separation is cancer, mainly by the aggregation of mutant variants of the tumor suppressor protein p53, which are frequent in malignant tumors. Carcinogenic mutations are located in the DNA-binding domain of p53, causing misfolding and condensation. In turn, condensation of p53 results in amorphous solid condensates and amyloid fibers (Petronilho et al., 2021).

2.7. Viral condensates

Viruses resort to protein condensation for replication and progeny assembly. Over the years viral condensates have been named viral inclusions, viral factories, virosome, viroplasm, mini-nuclei, aggresomes, etc. Many of these condensates are connected to organelles: mitochondria (flock house virus); lysosome (Semliki Forest and rubella virus), peroxisome (tomato bushy stunt virus); Golgi complex (Kunjin virus); and ER (hepatitis C virus, dengue, severe acute respiratory syndrome coronavirus-2) (Etibor et al., 2021). Other are connected to membraneless condensates or in the cytoplasm: microtubule organizing center (Poxviridae, Iridoviridae and Asfaviridae); cytoplasm (rhabdoviruses and filoviruses) (Nikolic et al., 2017).

The vast and rapidly expanding field of protein condensation in viral life cycle and control of virus-host interactions has been comprehensibly reviewed (Brocca et al., 2020; Lopez et al., 2021). Here, we will describe only one of the many examples of the close connection between liquid condensation and viral lifecycles. In coronaviruses, capsid and genome assembly occurs in dynamic, cytoplasmic *foci* in proximity to membrane structures, in agreement with phase separation having a role in replication or packaging. Coronaviruses have large RNA genomes whose packaging excludes host RNA and viral subgenomic RNAs. Viral replication and gRNA packaging depends on the N-protein, which possesses RBDs and IDRs, typical features of proteins that promotes condensation. The N-protein forms cytoplasmic, liquid-like condensates *in vitro* and in cells, and its phase-separation depends of RNA sequence and structure (Iserman et al., 2020).

2.8. Extracellular condensates

Extracellular deposits of proteins are ubiquitous. These include but are not limited to collagen, blood clot forming fibrin, insect elastic matrix protein resilin, hinge ligament of bivalve molluscs abductin, spider and insect silks, matrix proteins of squid suckers, attachment fibers and adhesives of mussels, and bacterial biofilms (Muiznieks et al., 2018; Urosev et al., 2020; Seviour et al., 2020). Only two representative extracellular protein condensates, elastin and silk, will be briefly described.

Elastin, a key component of the vertebrate extracellular matrix, is a fibrillar protein that endows resistance to mechanical strain and elasticity to different tissues. Completely formed during development, elastin fibers last the adult lifetime and are not renewed. The first step in the assembly of the elastin network is the condensation of crosslinked tropoelastin, a 70-kDa protein with non-polar, glycine-rich, low-complexity IDDs. After secretion and during the initial phase separation, tropoelastin forms a liquid condensate with other proteins, including fibrillins, fibulins, emilin-1, microfibril-associated glycoprotein-1, and latent TGF-beta binding protein. Tropoelastin monomers deposit in the condensate and become chemically crosslinked by lysyl oxidase, a copper-dependent amine oxidase, to form an insoluble network (Yanagisawa and Davis, 2010; Muiznieks et al., 2018).

Spider silk materials are semi-crystalline condensates of ordered domains containing spindroin, which is a large polypeptide with a central repetitive domain and one small globular domain at each end. Whereas the central repeat sequence endows the silk fiber its mechanical properties, the globular domains have a role in the process of silk assembly. Before spinning, spidroin forms a liquid condensate inside the sac of silk glands. As spidroin travels along the spinning duct, it experiences changes in pH, salt composition, and dehydration, as well as the effects of shear forces. As a result of these stimuli, spindroin converts from a largely unfolded state into solid fibers, with a hierarchical arrangement of aligned nano-crystalline β sheets immersed in a more amorphous background of protein chains (Walker et al., 2015; Malay et al., 2020).

3. Protein conformation and phase separation

3.1. Types of conformation and phases

A comprehensive approach to protein conformation encompasses a wide range of different structural entities dwelling in a variety of phases. The entities are ordered and disordered domains interacting homo- and hetero-typically. The phases span a range of material properties: dilute solutions, liquid condensates, gels, amorphous solids, ordered solids, and crystals (Wunderlich, 1999; Haas and Drenth, 1999; Van Der Lee et al., 2014; Goetz and Mahamid, 2020; Soranno, 2020; Sawaya et al., 2021).

3.2. Factors that promote phase separation

Temperature and protein concentration are the most important variables driving phase separation: enthalpy, entropy, and heat capacity are functions of temperature, and concentration provides the spatial proximity of protein chains that stabilizes condensed phases. In addition, chemical composition modulates phase separation.

Phases are connected by transitions. For instance, demixing originates liquid condensates from saturated solutions upon cooling, and liquid condensates may transform in gels, ordered or amorphous solids, and crystals with time. It should be kept in mind that phases *in vivo* are far from equilibrium, and their separation is regulated by changing the concentrations of interacting macromolecules and their mutual affinity. Protein concentration can be changed via protein translation, degradation or transport, whereas affinity is changed via posttranslational modification or genetic manipulation (Patel et al., 2015; Fox et al., 2018; Mukherjee et al., 2020).

A commonly held belief is that phase separation is exclusive of particular protein sequences or disordered conformations. However, any sequence or conformation is susceptible to phase separation, provided that the appropriate concentration, temperature, and solvent condition is reached (Martin and Mittag, 2018; Hardenberg et al., 2020; Miskei et al., 2020; Horvath et al., 2020; Poudyal et al., 2022). In this regard, phase separation of properly folded proteins was studied *in vitro* long before than *in vivo* (Lerman et al., 1966; Siezen et al., 1985; Thomson et al., 1987; Broide et al., 1991; Berland et al., 1992).

The concentration and material properties of the phases are further influenced by the number of macromolecular components. Whereas simple temperature-concentration phase diagrams based on polymer chemistry theory can be used to model the phase behavior of binary systems, a much more elaborated scenario is set forth for multicomponent systems in the cell (Riback et al., 2020). In cellular, multicomponent systems, 'scaffold' proteins, which phase-separate by their own, drive phase separation of 'client' proteins (Banani et al., 2016). In turn, client proteins can pervade the mutual condensate or associate to its surface (Kelley et al., 2021).

Phase diagrams conveniently display the relationship between phases, concentration, and temperature (or temperature-related variables) (Thomson et al., 1987; Broide et al., 1991; Berland et al., 1992; Muschol and Rosenberger, 1997; Haas and Drenth, 1999; Grouazel et al., 2006; Cardinaux et al., 2007; Dumetz et al., 2008; McManus et al., 2016; Shin and Brangwynne, 2017; Adamcik and Mezzenga, 2018; Holehouse and Pappu, 2018a; Yadav et al., 2019; Alberti et al., 2019; Soranno, 2020; Dignon et al., 2020). A generic phase diagram for proteins in the temperature–concentration plane is shown in Fig. 1. In the single phase regime, two regions are separated by the solubility (saturation) curve: the undersaturated and the supersaturated liquid regions. Liquid condensates, gels, amorphous aggregates, fibers, and crystals may emerge upon nucleation in the metastable, supersaturated region below the solubility curve. (Arakawa and Timasheff, 1985; So et al., 2016; Vecchi et al., 2020; Noji et al., 2021).

Since only supersaturation leads to phase separation, it is clear that there is a strong connection between protein concentration and phase separation. Indeed, phase separation (condensation) is the only way to increase protein concentration above the solubility limits. Protein concentration in gels, amorphous aggregates, and fibers can be considered independent of temperature; vertical lines mark the separation of these states in Fig. 1.

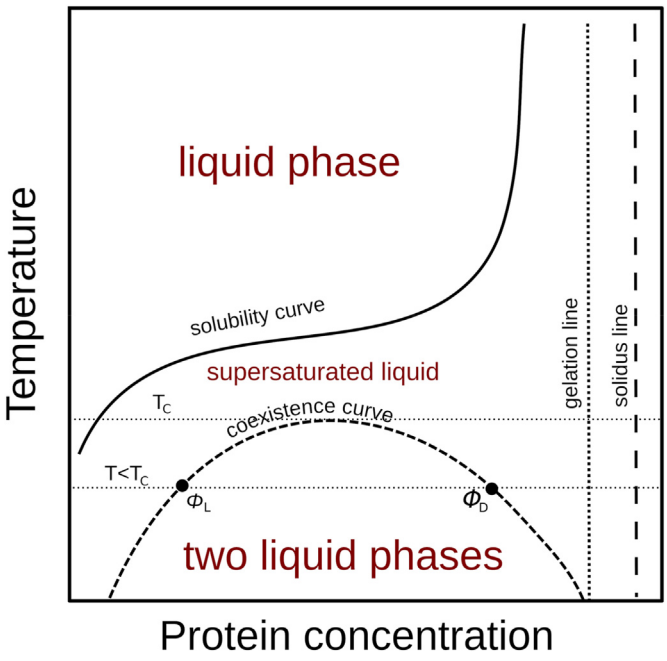

Fig. 1. Schematic protein-water phase diagram in the temperature–concentration plane. The sketch illustrates the behavior of a binary system with normal temperature dependence of the solubility, *i.e.*, the solubility increases with temperature. Protein concentration is represented as volume fraction (*Φ; see text*). Below the solubility curve, supersaturated solutions are metastable and eventually undergo transitions to the condensed liquid phase or to solid-like phases, such as gel states, crystalline states, amorphous solids, and fibers. The liquid-liquid coexistence curve (short dashes), also called binodal, maps the transition to the two-phases regime, where a liquid condensed phase coexists with a liquid dilute phase. The critical temperature (T_C) is the temperature above which the concentration differences between the two liquid phases vanishes and a homogeneous solution exists. At each temperature below T_C, the coexistence curve defines pairs of protein concentrations, Φ_L and Φ_D, which characterize the protein volume fractions of the light and dense phases, respectively. The concentrations of the light and dense phases remain constant for a given temperature and are independent of the total protein concentration of the system. What changes with the total concentration of the system is the relative volume of each phase. Thus, the left arm of the coexistence curve maps the volume predominance of the light phase, whereas at the right arm predominates the volume of the dense phase. This remarkable behavior explains why at low total concentrations the system exhibits droplets of highly concentrated protein dispersed in a dilute phase, whereas at high total protein concentration droplets of dilute protein are dispersed in a dense phase. The gelation line (dots) represents the protein concentration of gel phases. The solidus line (long dashes) define the protein concentration of crystals, amorphous aggregates and fibers.

A coexistence curve, also called binodal, is the boundary between the single-phase and the liquid condensate regions (Fig. 1). The temperature coordinate tangent to the coexistence curve defines the critical temperature (T_c), at which the protein concentration of the two separated phases is the same, *i.e.*, is the highest temperature at which phase separation occurs. Below T_c, each temperature coordinate intersects the coexistence curve at two concentration values, which are the concentrations of the dilute (light) and dense phase, respectively. For simplicity and unless otherwise indicated, in this review we only discuss phase separations with upper critical-solution temperature, which is frequently observed in proteins. However, phase separations with lower critical-solution temperature have been also characterized. (Martin and Mittag, 2018).

Thermodynamic equilibrium constrains the concentration of the two separated phases at each temperature to the values on the coexistence curve. Concomitantly, due to mass conservation, the relative volume of the two separated phases changes with the total concentration of the macromolecule in the system: on the right arm of the coexistence curve, a light phase is dispersed in the predominant, dense phase, whereas the opposite happens on the left arm.

In phase separation, the concentration of each component is advantageously treated as volume fraction (Φ, the fraction of the total volume occupied by each component). By definition, $\Phi = C \times V_s$, where C and V_s are the concentration and specific volume of the components, respectively. Unitless Φ values allow easier appreciation of intermolecular distances. For instance, the ideal densest packing of spheres corresponds to $\Phi = 0.74$, at which value each sphere is at contact distance with twelve nearest spheres. However, for entropic reasons, random hard-sphere packing of fluids corresponds to Φ values of approximately 0.5 (Manoharan, 2015). In phase-separated liquid condensates, typical Φ values are approximately 0.3 (see below). In most protein crystals, Φ ranges 0.27–0.65 (Matthews, 1968). However, in some extreme cases, crystal unit cells contain about 15% solvent, which equals to a Φ value of 0.85. At $\Phi = 0.3$, the distance between protein molecules approaches the molecular diameter, which makes possible the intermolecular contacts stabilizing the separated phases. The number of intermolecular contacts, as expected, increases with Φ values and with the complimentary shape of the molecules (Lawrence and Colman, 1993).

Notwithstanding the usefulness of Φ values, a common ground for the analysis of phase separation and protein conformation may be found considering the change in molecular accessible surface area (ASA) of the corresponding transitions. In phase separation, the change in ASA is related to the change in Φ values. Furthermore, there is a direct connection between ASA and the state variables of protein thermodynamics, which may allow to rationalize protein conformation, binding and phase separation using the same metrics (Hilser et al., 1996; Ikenoue et al., 2014; Kardos et al., 2004).

The general considerations made in this section have mostly to do with simple binary systems. However, they provide the basic conceptual framework needed to approach more complex systems found in cellular and extracellular environments.

4. Liquid condensates

4.1. Thermodynamics of liquid condensation

Dilute protein solutions lack of persistent spatial order or symmetry. In these, the diffusion of each component is little disturbed by intermolecular interactions, and protein concentration is thermodynamically controlled not to exceed the solubility limit. Accordingly, the thermodynamics of dilute protein solutions is mainly concerned with conformational changes and binding of individual molecules. Two main terms define the entropy of dilute protein solutions: the degree of freedom of the conformation of the chains and the number of water molecules organized on the protein surface. On the other hand, the main enthalpic terms arise from molecular surface interactions: water–water, water–protein, and protein–protein interactions. Entropic and enthalpic contributions follow a complex pattern with temperature, leading to the enthalpic–entropic compensations that define protein conformation (Privalov, 2007).

Due to their higher concentration, the distinguishing feature of condensed liquids is an exacerbated protein–protein intermolecular interaction. In addition, liquid condensates feature long-range molecular disorder concomitantly with elastic response to deformation at short timescales (viscoelasticity); that is, they can adopt spheroidal shapes, fuse, coalesce and drip, driven by surface tension or by external forces. Within liquid condensates, protein chains are highly mobile and rapidly exchange with the dilute phase; however, diffusion of proteins within the dense phase is considerably slower than in the dilute phase (Hyman et al., 2014; Brady et al., 2017; Ruff et al., 2018; Alberti et al., 2019; Yewdall et al., 2021; Abyzov et al., 2022).

The coexistence curve (binodal) maps the concentrations of light and dense phases (Φ_L, and Φ_D, respectively) at different temperatures (Fig. 1). For simple binary systems and in the proximity of the critical temperature (T_C), an empirical equation can be fitted to the coexistence curve,

$$T = T_c\left(1 - \alpha\left|\frac{\varphi C - \varphi}{\varphi C}\right|^{1/\beta}\right) \quad \text{Eqn. 1}$$

in which Φ is a pair (Φ_L,Φ_D) for each temperature T, Φ_C, α, and T_C are protein specific adjustable parameters, and $\beta = 0.325$ is the critical exponent for binary demixing from renormalization-group theory (Broide et al., 1991; Muschol and Rosenberger, 1997; Honda and Matsuyama, 1999; Platten et al., 2015; Martin et al., 2021).

If sufficient pure protein is available, the experimental determination of Φ_L, and Φ_D is straightforward. Several techniques can be used to that end; however, separation by centrifugation allows direct assessment of concentrations and volumes of the two coexisting phases (Grouazel et al., 2006; Milkovic and Mittag, 2020). More elaborated techniques can be utilized if the supply of pure protein is scarce (McCall et al., 2020).

Although the overall shape of the coexistence curve can be captured by power functions like *Eqn.* 1, a more elaborated treatment is needed to gain insight into the thermodynamics of liquid-liquid phase separation. The transformation of a low density phase into a high density phase entails entropy loss, which must be compensated by enthalpic contributions from molecular interactions. Flory–Huggins lattice models capture the enthalpic-entropic contributions to liquid condensation (Huggins, 1941; Flory, 1942; Rubinstein et al., 2003). In the simplest formulation, the free energy in these models can be defined as

$$\Delta G = K_b T\left[\frac{\varphi}{\nu_e} In\varphi + (1-\varphi) + X\varphi(1-\varphi)\right] \quad \text{Eqn. 2}$$

where χ is a temperature-dependent parameter that accounts for the strength of the interactions between different molecular species, ν_e is a temperature-dependent, effective volume corresponding to the phase-separating component and relative to the molecular volume of the solvent, Φ is the volume fraction of the macromolecule, and k_B is the Boltzman constant. In this equation, the two left and the right terms represent the entropic and enthalpic components of ΔG, respectively (Curtis et al., 2001; Dumetz et al., 2008; Spruijt et al., 2010; Wolf et al., 2014; Brady et al., 2017; Wei et al., 2017; Martin and Mittag, 2018; Ruff et al., 2018; Li et al., 2018; Shapiro et al., 2021).

Since the entropy of mixing strongly disfavors phase separation, enthalpic terms incline the balance toward the association (demixing) of separating molecules. This association is remarkable because it takes place between disordered as well as folded protein molecules, which poses the very interesting question of how low affinity and low specificity interactions accumulate enough strength as to tip the equilibrium toward phase separation. Intuitively, one is led to think that these interactions are numerous, compensating weakness with number. However, this issue is currently under intense investigation.

Simulated $\Delta G(\Phi,T)$ curves using *Eqn.* 2 are shown in Fig. 2. Equilibrium implies that the chemical potential ($\mu = \partial\Delta G/\partial\Phi$) in and out of the condensates is the same, a condition represented in each curve by color matching dots (Fig. 2A). In turn, these dots define the coexistence curve in the phase diagram (Fig. 2B). Below the coexistence curve, the system phase separates, either spontaneously or after a nucleation process. In the region close to the coexistence curve, the system is metastable and phase separation is delayed by a kinetic barrier upon the occurrence of nucleation events. The metastable region of the phase diagram is delimited by the coexistence curve and the spinodal curve ($\mu = \partial^2\Delta G/\partial\Phi^2$; not shown) (Shapiro et al., 2021). Below the spinodal curve, the system is unstable and phase separate abruptly. In practice, points on the coexistence curve are determined experimentally and used to define by numerical

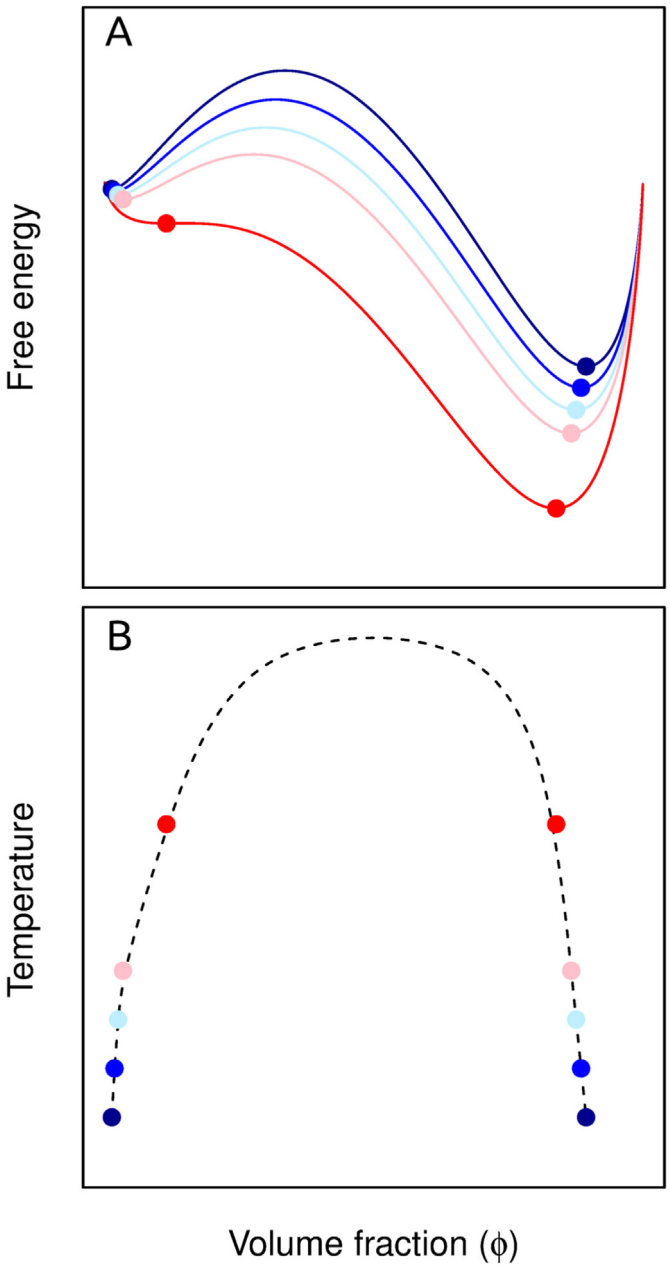

Fig. 2. Simulated free energy curves and phase diagram of liquid-liquid phase separation. (*A*) Free energy isotherms were calculated using *Eqn.* 2 assuming $\chi(T) = a+b/T$ and $T = 300$ K (dark blue), $T = 320$ K (blue), $T = 340$ (light blue), $T = 360$ K (light red), $T = 370$ K, (red). Dots mark points of equivalent chemical potential (equivalent first derivative of the free energy) and define the single common tangent of each curve. (*B*) The phase diagram defined by the points in panel *A*. The dashed line was drawn only to guide the eye, and it estimates the coexistence curve (binodal). (For interpretation of the references to color in this figure legend, the reader is referred to the Web version of this article.)

calculations the parameters of the respective free energy curves (Petsev et al., 2003; Brady et al., 2017; Martin and Mittag, 2018; Martin et al., 2021; Fritsch et al., 2021).

Although minimalist Flory–Huggins models are adequate for a preliminary analysis, more elaborate treatment is needed to explain accurately the experimental data in protein systems with significant conformational fluctuations and sequence effects. In these cases, additional terms accounting for effective macromolecular volumes and inter- and intra-chain interactions need to be included (Overbeek and Voorn, 1957; Wei et al., 2017; Berry et al., 2018; Zhou et al., 2018; Shapiro et al., 2021; Biswas et al., 2021). Likewise, multicomponent and *in vivo* systems demand specific treatments (Saha et al., 2016; Fritsch et al., 2021). Extensions of the Flory–Huggins model were recently reviewed (Shapiro et al., 2021).

An important consequence of the chemical potential equality of demixed phases ($\mu_L = \mu_D$) is that Φ_L and Φ_D are independent of the total (mixed) macromolecule concentration (Φ_T), and because the total volume (V_T) of the system is constant, the only degree of freedom at a given temperature is the relative volume of the demixed phases. The volume balance implies the following:

$$V_T = V_L + V_D \qquad \text{Eqn. 3}$$

and

$$V_L\,\varphi_L + V_D\,\varphi_D = V_T\,\varphi_T = \nu_{prot} \qquad \text{Eqn. 4}$$

where ν_{prot} is the total molecular volume of the protein in the system. It must be kept in mind that the above considerations apply only to simple binary systems *in vitro*. The situation is more complex in multicomponent systems, such as those found in living cells and which contain complex mixtures of multivalent macromolecules whose concentration is metabolically regulated (Chattaraj et al., 2021).

4.2. Liquid condensation of folded proteins

The first report of temperature-induced liquid condensation of a protein was in 1977 for lysozyme (Ishimoto and Tanaka, 1977), a well-characterized 14.3-kDa folded protein; a decade later, Taratuta et al. reported a complete phase diagram for this protein (Taratuta et al., 1990). As a prototypical example, Cardinaux et al. found that lysozyme at 15 °C, 0.5 M NaCl, and pH 7.8 was 32 and 5.6 mM in the dense and light phases, respectively (Cardinaux et al., 2007); i.e., in the condensate, lysozyme was concentrated by a factor of five. Using the protein specific volume, it can be calculated that Φ_L, and Φ_D were 0.06 and 0.33, respectively.

Simple math will help to get a mental picture of the spatial arrangement of lysozyme molecules in its condensate. Avogrado's number imposes that in a 32 mM solution there is one lysozyme molecule per 5.2×10^4 Å^3. To estimate the center-to-center distance between nearest lysozyme molecules, it is necessary to choose a model for their spatial arrangement. For instance, the random closest-packing model predicts that on average there are six closely-distanced neighbors (Torquato, 2018). A similarly efficient packing is that of a body-centered cubic cell, for which the center-to-center closest distance can be analytically calculated. For 32 mM condensed lysozyme, the calculation indicates a closest distance of 40.7 Å. This dense phase closest distance is consistent with the lysozyme experimental hydrodynamic diameter of 37.8 Å (Parmar and Muschol, 2009) and implies that, on average, six nearest-neighbors are at binding distance of each other and separated by less than a water molecule diameter (2.8 Å). Therefore, a significant fraction of these contacts should realize transiently to explain the rheological properties of the condensate (Cardinaux et al., 2007) and the establishment of multiple short-range attractive forces between protein molecules that drive the demixing of the system (Petsev et al., 2003).

Another folded protein engaging in binary liquid-phase separation is γ crystallin. It was studied early for its involvement in cataratogenesis, and Φ_L and Φ_D values of 0.05 and 0.40, respectively can be inferred from its phase diagrams (Broide et al., 1991). In this case, γ crystallin condensate became concentrated by a factor of eight. Using the same considerations as in the lysozyme case, a nearest-neighbor distance of 43.0 Å can be calculated for γ crystallin, and this value can be contrasted with its hydrodynamic diameter of 42.0 Å. Again, the difference between these two values suggests that a single-molecule water layer separates adjacent γ crystallin molecules in the condensed phase.

The LLPS of bovine pancreatic trypsin inhibitor (BPTI) —a disulfide-

bridged, folded protein— was also thoroughly characterized (Grouazel et al., 2006). At 23 °C, BPTI became phase-separated with Φ_L and Φ_D values of 0.02 and 0.34, respectively, which represents a 18 times higher concentration in the dense phase relative to the light phase. In concentrated solution, dense liquid phase, and crystals, BPTI formed a roughly spherical homo decamer of about 65.4 Å diameter. Number density analysis indicates that in the condensed liquid phase, six BPTI nearest neighbors decamers are at a center-to-center distance of 72.4 Å. That is, the separating distance between decamers is 7 Å (less than three water molecule diameters). Therefore, based solely in spatial proximity consideration, the engagement of BPTI decamers in multiple transient homotypic interactions is to be expected.

4.3. Liquid condensation of disordered domains

The liquid condensates described above are from folded proteins, which have precisely defined molecular shapes and dimensions. Instead, disordered protein domains populate ensembles of fluctuating structures, whose shapes and dimensions can be inferred only statistically.

It is customary to represent globularly folded proteins as ideal spheres that exclude one another. For disordered protein chains, the spherical representation remains useful; however, it needs to be redefined as an average spherical volume of the chain conformational ensemble. Importantly, since folded chains are characterized by maximal compaction, the volume that includes a disordered chain is larger than the volume of an equivalent folded chain, and the volume excess can be partially occupied by a nearest chain. In condensed phases, whereas globular folded proteins 'touch' one another, disordered proteins chains overlap (or interpenetrate) up to different degrees of entanglement, enmeshing or fibrillation (Fig. 3). The concept of overlapping macromolecular concentration rationalizes the degree of interpenetration of the average volumes pervaded by each macromolecule (Ying and Chu, 1987). A simple geometrical formula can be used to estimate the degree of overlapping of spheres,

$$V_{ovl} = \frac{1}{12}\pi(4R + d)\,(2R - d)^2 \qquad \text{Eqn. 5}$$

where V_{ovl} is the common volume shared by two overlapping spheres of radius R at the center-to-center distance d. In practice, the experimental hydrodynamic radius (R_h) measured by a biophysical technique can be used to calculate the overlapping volume; however, an accurate R_h measurement can only be performed in dilute solutions and the extrapolation to a condensed phase should be cautiously interpreted.

Following, we will review highly significant advances achieved recently in the study of liquid condensates of disordered protein domains for which the concentration in the condensed phase was directly determined.

4.3.1. Ddx4

Ddx4, an RNA helicase required during spermatogenesis, is the primary protein constituent of the germ-cell-specific membraneless organelle nuage. It features a central DEAD-box, RNA-helicase domain and intrinsically disordered N- and C-termini. These termini are LCDs with characteristic repeats of 8–10 residues of alternating net charge and FG, GF, RG, and GR motifs. *In vitro* phase separation of the N-terminal LCD of Ddx4 (236 residues, Ddx4N1) was thoroughly characterized using NMR techniques in the pioneering works of Forman-Kay and colleagues (Nott et al., 2015; Brady et al., 2017). The measured concentration of Ddx4N1 in the *in vitro* liquid condensate was 380 mg/ml (30 °C; 14.7 mM), and the condensate was in contact with a 7 mg/ml (0.26 mM) dilute phase. Using the theoretical specific volume of Ddx4N1 estimated from the sequence (Harpaz et al., 1994), these concentrations translate into Φ_D and Φ_L values of 0.26 and 0.005, respectively, that is there was a 50 times concentration difference between the two phases. Importantly, the condensate Φ_D value of 0.26 was experimentally validated by NMR measurements of water content. The calculation of the number density of Ddx4N1 indicates that in the liquid condensate the center-to-center distance between Ddx4N1 molecules was 52.7 Å. A 'touching', center-to-center distance between Ddx4N1 molecules of 62 Å can be calculated from the R_h measured by NMR in the dilute phase. The difference between the two center-to-center distances reflects the degree of spatial overlapping of Ddx4N1 molecules in the condensate. Using *Eqn. 5,* the center-to-center distance and the R_h indicated above, the calculated overlapping volume for Ddx4N1 is 3.2% per contact. That is, based in the degree of overlapping, the Ddx4N1 chain entanglement is moderate; nonetheless the measured translational diffusion coefficient of Ddx4N1 in the condensed phase is equivalent to that of a 500 nm particle.

The overlapping volume gives only a hint of the extent of the intermolecular interactions; high resolution methods are needed to assess the quality and strength of these interactions. In this regard, NMR results showed the importance of Phe and Arg cation–π and π–π intermolecular interactions in driving the phase separation of Ddx4N1.

Another very interesting aspect in the investigations of Forman-Kay and coauthors is the demonstration that Ddx4N1 propensity to phase separation is rooted in its sequence, not in its intrinsic disorder. Disordered Ddx4N1 with scrambled sequence and Ddx4N1$_{14FtoA}$, a variant in

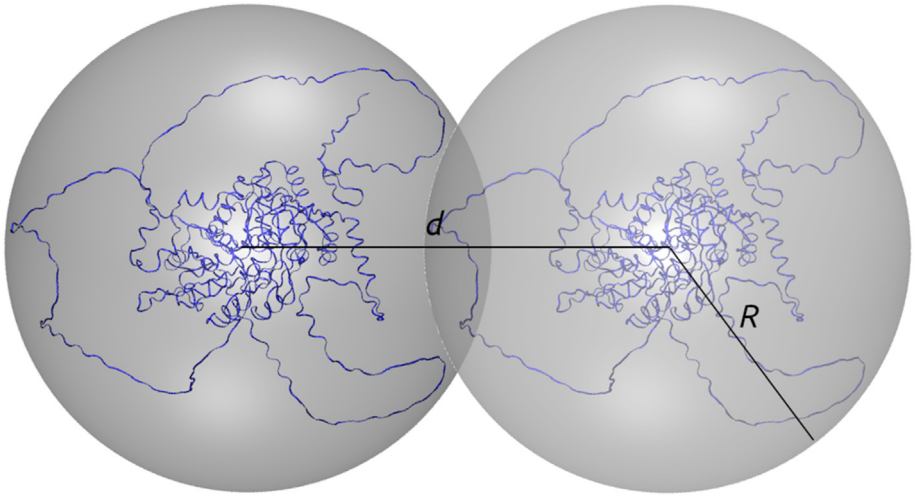

Fig. 3. The concept of overlapping volume. Two chains combining folded and disordered domains are embedded in the minimal spherical volume that include all the chain atoms. The volume intersection of the two spheres is the geometrical lens, and the larger this volume the higher the probability of intermolecular interaction and entanglement. The overlapping volume (darker gray) can be calculated from the radius of the sphere (R) and the center-to-center distance (d) using *Eqn. (5)*.

which 14 Phe residues were changed to Ala, phase separated at temperatures much lower than wild type Ddx4N. Likewise, disordered Ddx4N1$_{24RtoK}$, a variant having 24 Arg residues replaced with Lys residues, did not phase separate under the conditions tested.

4.3.2. Caprin

Caprin-1 is an RNA-binding protein that contributes to the formation of stress and neuronal granules. A C-terminal region of caprin-1 comprising residues 607–709, caprin-1-LCD, is a disordered LCD with sequence features that correspond to PLDs: a typical amino acid composition and a striking enrichment of glutamine and asparagine residues (Lancaster et al., 2014; Fomicheva and Ross, 2021). NMR studies of caprin-1-LCD provided further insights into the arrangement of disordered protein chains in liquid condensates.

Depending on the ionic strength and temperature, phase diagrams of caprin-1-LCD showed condensed phase concentrations ranging from 14 to 36 mM. At 25 °C and 600 mM NaCl, protein concentrations were approximately 0.8 and 36 mM, Φ_L and Φ_D values of 0.006 and 0.28, for the dilute and dense phases, respectively; *i.e.*, phase separation brought about a forty-fold concentration increase (Wong et al., 2020; Kim et al., 2021).

Based on the number density of 36 mM caprin-1-LCD, the center-to-center distance to the nearest-neighbor can be estimated as 39.1 Å; whereas the estimation of the minimal hydrodynamic diameter of the disordered molecule is about 43 Å. Applying *Eqn. (5)*, the overlapping volume results in 1% per contact. Thus, the degree of entanglement is moderate and similar to that of Ddx4N1 analyzed above. Repeating the calculations for a 14 mM caprin-1-LCD, the lowest concentration reported for the condensate, one arrives at a center-to-center distance to the nearest-neighbor of 53 Å. Thus, with a diameter of 43 Å, chains are 10 Å apart and do not overlap. This important result underscores that persistent entanglement is not mandatory for liquid phase separation of disordered domains. In this regard, disordered and folded domains are alike.

As seen above for Ddx4N1, intrinsic conformational disorder *per se* does not justify phase separation of caprin-1-LCD: caprin-1-LCD$_{15Rto15K}$ (in which all Arg are replaced by Lys) did not phase separate under the conditions tested (Wong et al., 2020). In this connection and because Arg to Lys substitutions preserve the residue charge, the resistance of caprin-1-LCD$_{15Rto15K}$ to phase separate was attributed to the elimination of intermolecular π interactions of the guanidinium group (Vernon et al., 2018).

Further analysis established that not all Arg residues of caprin-1-LCD were equally important, as four arginine residues located in the N-terminal region contributed the most to phase separation. The importance of arginine residues was also demonstrated by the effect of sodium pyrophosphate, a strong guanidinium binder. Phase separation of caprin-1-LCD was promoted by sodium pyrophosphate at concentration as low as 3 mM, which is two orders of magnitude less than the effective concentrations of sodium chloride or phosphate. In addition, cross peaks in 3D NMR spectra showed distinct binding of ATP-Mg to arginine-rich, N- and C-terminal, caprin-1 sequences (Kim et al., 2021).

To garner site-specific information on intermolecular interactions in the condensed state of caprin-1-LCD, NMR experiments with high sensitivity and resolution were developed. Overall, Arg and Gly residues, and α-hydrogen atoms were particularly important in establishing interchain interactions. Also, distinct intermolecular interactions linking aromatics residues with Arg and Gln amides, and with aromatic backbone protons from a second chain were observed for the aromatic-rich regions of the chains. More in detail, NOE experiments established that specific sequences in the aromatic region of caprin-1-LCD showed an enhancement of interchain contacts. The importance of these sequences for liquid phase separation was confirmed by three-residue stretch mutagenesis experiments. On the other hand, NOE experiments demonstrated that intramolecular contacts were primarily between sequential-residues, and thus the picture emerging from the NMR characterization showed adjacent chains interacting with each other all along their lengths but with distinct sequence preferences (Kim et al., 2021).

4.3.3. Fus

The RNA-binding protein Fused in Sarcoma (FUS) plays a role in RNA processing and localizes both to cytoplasmic ribonucleoprotein granules and transcriptionally-active nuclear *puncta*. FUS, probably the most well-studied condensing protein, has been involved in protein aggregation in the degenerative diseases ALS and FTD, and about 30 FUS-related human protein families (FET) have been described (Sun et al., 2011; King et al., 2012; Patel et al., 2015; Molliex et al., 2015).

FUS, features a disordered LCD and a RBD, and its N-terminus classifies as a PLD. Liquid phase separation of FUS is enhanced by the interaction of tyrosine and arginine residues from the RBD and the PLD. Notably, the rheological properties of the liquid condensates are modulated by serine, glutamine, and glycine residues (Wang et al., 2018). FUS N-terminus (FUS-LCD) spans a 163-residue sequence capable of liquid phase separation *in vivo* and *in vitro* (Sun et al., 2011). Insightful works by Fawzi and colleagues (Burke et al., 2015; Monahan et al., 2017; Murthy et al., 2019) indicated that in mixed and condensed phases FUS-LCD was highly disordered and dynamics, lacking long-term intermolecular contacts. Nevertheless, the translational diffusion of FUS-LCD in the condensed phase was approximately 500 times slower than in the dispersed phase, implying the presence of significant short-term intermolecular interactions. Interestingly, in the condensed phase the solvent diffused six times slower than in the dispersed phase.

Fawzi and colleagues reported that in a FUS-LCD condensate isolated by centrifugation the protein concentration was 27 mM ($\Phi_D = 0.32$). The number density and the mass concentration allow us to estimate a center-to-center nearest-neighbor distance of 42.6 Å. In addition, the reported translational diffusion coefficient in the dilute phase is consistent with a hydrodynamic diameter of 51.2 Å. Assuming that the FUS-LCD hydrodynamic diameter is the same in both phases, it can be concluded that FUS-LCD chains partially overlap in the condensed phase. According to *Eqn. (5)*, the overlap is 4% per interaction, implying a moderate chain entanglement as in the cases of Ddx4N1 and caprin-1 described above.

Based in their NMR evidence, Fawzi and colleagues concluded that transient intermolecular contacts were formed promiscuously along FUS-LCD chains, with no evidence for persistent assemblies or significant conformational changes. These interactions would be short-lived and low-populated, as to permit the fluctuation of the chain as a whole and nevertheless to restrict local motions of the peptide backbone. Additionally, the author's NMR spectra, all-atom simulations, and mutagenesis studies showed that FUS-LCD condensed state was stabilized by hydrogen bond, hydrophobic, and π/sp^2 contacts from several residue types, albeit the contribution of glutamine and tyrosine hydrogen bonding was particularly noticeable. Interestingly, it has been pointed out that π–π interactions, as those arising from sp^2-hybridized atoms, are relevant features of many protein condensates (Vernon et al., 2018).

As in the cases of Ddx4N1 and caprin-1-LCD, FUS-LCD condensation depends more on sequence details than on intrinsic disorder: FUS-LCD 12E, a variant with 12 serine or threonine to glutamate mutations did not undergo condensation despite being disordered. Similarly, two variants with four pairs of glutamine to serine substitutions showed decreased partitioning into the condensed phase. Contrarily, a variant with 12 serine-to-glutamine substitutions, exhibited increased partitioning. Furthermore, substitution of 24 residues of tyrosine to phenylalanine led to aggregation, suggesting that the sequence was precisely tuned to produce liquid-like behavior.

The condensed-phase concentration of full length FUS-GFP measured by quantitative phase microscopy was 4.2 mM ($\Phi_D = 0.23$) (McCall et al., 2020), from which we deduce a center-to-center intermolecular distance of 80 Å. Since the FUS-GFP fusion contains folded and disordered domains, it is difficult to estimate its hydrodynamic diameter. However, we calculate a tentative diameter of 156 Å from the 3D model predicted by AlphaFold (Tunyasuvunakool et al., 2021). Thus,

applying *Eqn. (5)*, the overlap of pervaded volume is 30% and the degree of entanglement high.

4.3.4. hnRNPA1

Heterogeneous nuclear ribonucleoprotein A1 (hnRNPA1) is a 371-residue protein involved in packaging of pre-mRNA into hnRNP particles, transport of poly(A) mRNA, and splice-site selection. It is mostly disordered, except for two N-terminal, RNA-recognition-motif (RRM) domains and a central, RNA-binding RGG-box. The C-terminal half of the protein (residues 186–320, A1-LCD) encompasses one LCD that qualifies as a PLD and drives phase separation.

Martin et al.used NMR spectroscopy to characterize prominent interactions in conformational ensembles of A1-LCD (Martin et al., 2020). In the absence of persistent structure, NOEs gave evidence of transient clustering among aromatic residues (F/Y). Since A1-LCD is enriched in evenly distributed aromatic residues, the authors hypothesized that these residues would function as 'stickers' establishing intrachain interactions. To test the hypothesis, they measured the radius of gyration (R_g) of A1-LCD variants and found that the degree of compaction of the chain was a function of the aromatic composition. Similar results were obtained using all-atom molecular simulations.

Next, the authors developed a bead model for predicting the phase behavior of A1-LCD using a lattice-based coarse-grained description, in which the sticker beads correspond to the aromatic residues whereas the 'spacer' beads correspond to the non-aromatic residues. Once parameterized for the strengths of the sticker-sticker, sticker-spacer, and spacer-spacer interactions, this model accurately reproduced experimental and simulated R_gs, and, more importantly, the parameterized stickers-and-spacers lattice model was used to perform Monte Carlo simulations showing that phase separation occurred in a sequence-, concentration-, and temperature-dependent manner. Accordingly, binodals calculated from the simulations showed the relationship between the number of aromatic stickers and the phase behavior of A1-LCD. Importantly, the binodals predicted from the lattice-based stickers-and-spacers model were in agreement with those determined experimentally.

The coexistence curves of A1-LCD variants experimentally determined by Martin et al. permits the evaluation of the extent of intermolecular interaction in the condensate. The concentration of wild type A1-LCD in the dense phase was 35 mM ($\Phi_D = 0.30$), a 390-fold concentration increase relative to the dilute phase. Based in the number density, we calculate a center-to-center distance of 41.3 Å. In parallel, the average hydrodynamic diameter estimated from SAXS measurements was 67.4 Å. Applying these values to *Eqn. (5)*, we calculate that the overlap volume is 20%, which suggests a substantial degree of molecular entanglement.

4.3.5. hnRNPA2

Homologous to hnRNPA1, hnRNPA2 is a 341-residue protein that forms inclusions bodies in multisystem proteinopathies (King et al., 2012). Physiologically, hnRNPA2 is involved in mRNA transport. It contains two folded RNA recognition motif domains and one disordered C-terminal PLD (hnRPA2 LCD; residues 190–341).

Ryan et al. reported that urea solutions of concentrated hnRPA2 LCD rapidly phase-separated at room temperature upon dilution into a non denaturing buffer, but this phase separation progressed reversibly to a gel-like state (Ryan et al., 2018). At 65 °C, the condensed phase remained liquid, allowing its bulk isolation and biophysical study. In the same work, it was reported that hnRPA2 LCD concentration in the condensate was approximately 440 mg/mL (30.6 mM; $\Phi_D = 0.30$). In addition, NMR pulsed-field gradient diffusion experiments established for hnRNPA2 LC a hydrodynamic diameter of 57.8 Å. Based in these results, we calculate that the typical nearest-neighbor-distance in hnRPA2 LCD condensate is 41.3 Å, and applying *Eqn. (5)* the overlapping volume is 11%. Thus, at this very high concentration and temperature, the entanglement in the condensed phase is moderate.

The chemical shift deviations, NMR spin relaxation enhancements, and paramagnetic relaxation enhancement experiments performed by Ryan et al. showed that contacts between hnRNPA2 LCD chains were of low affinity, non persistent, and widespread across the sequence. Importantly, the conformation of hnRNPA2 LCD in the condensate was similar to that in the dilute phase, and it was inconsistent with a regular structure such as found in amyloid aggregates.

4.3.6. TAF15

TAF15 is an RNA and ssDNA-binding protein that participate in transcription initiation. Except for a central, small RRM domain, most of its sequence is disordered. The N-terminal residues 1–180 of TAF15 constitute a PLD, and the C-terminal residues 181–589 conform with a RBD. Both, the entire protein and the isolated RBD phase-separated at low micromolar concentrations (Wang et al., 2018). By quantitative phase microscopy, McCall et al. analyzed liquid condensates of a TAF15 RBD construct fused to a SNAP tag (SNAP-TAF15 RBD) (McCall et al., 2020). They found that protein concentration in the condensate was 5 mM ($\Phi_D = 0.23$). The high molar concentration of SNAP-TAF15 RBD condensate implies a high number density, from which we estimate a nearest-neighbor center-to-center distance of 73 Å. The hydrodynamic behavior of the disordered molecule was not studied, which makes difficult to estimate its average hydrodynamic diameter. Nonetheless, it can be assumed that it behaves like a typical disordered protein with a diameter of circa 120 Å. With this assumption and applying *Eqn. (5)*, the overlapping volume of two interacting SNAP-TAF15 RBD molecules would be about 20%.

4.3.7. PGL3

PGL-3 is a *C. elegans* protein implicated in the formation of *P* granules. It contains six C-terminal RGG repeats that bind RNA (Saha et al., 2016; Schmidt et al., 2021). Using quantitative phase microscopy, McCall et al. found that the concentration of PGL-3 in the liquid condensate was 1.2 mM (McCall et al., 2020). The number density derived from this molar concentration indicates that the nearest-neighbor, center-to-center distance between molecules is 123 Å. Since PGL3 combines folded and disordered domains, estimating its hydrodynamic size is difficult; however, the AlphaFold model predicts that the minimal sphere that includes all PGL3 atoms has a 125-Å diameter. Thus, we conclude that PGL-3 molecules in the condensate are at touching distance from each other with a low degree of entanglement.

4.3.8. LAF1

The *C. elegans* protein LAF-1 belongs to the DDX3 family and contains an arginine/glycine-rich (R/G or RGG) domain implicated in phase separation and formation of *P*-granule-like droplets *in vitro* (Elbaum--Garfinkle et al., 2015). Wei et al. resorted to ultrafast-scanning fluorescence correlation spectroscopy (usFCS) to measure second virial coefficients, molecular diffusion coefficients, and binodals for LAF-1 and its intrinsically disordered RGG domain (Wei et al., 2017). At 125 mM NaCl, LAF-1 concentration inside the liquid droplets was 90 μM ($\Phi_D = 4.9 \times 10^{-3}$), in contact with a 1.6 μM ($\Phi_L = 8.7 \times 10^{-5}$) dilute phase. Surprisingly, the measured concentration was two orders of magnitude lower than that of typical liquid condensates. Interestingly, the binodal arms of the RGG domain alone are at mass concentrations similar to those of full length LAF-1, although the critical salt concentration is lower than that of full-length LAF-1.

Based on the AlphaFold model and assuming full unfolding, we estimate that the hydrodynamic diameter of LAF-1 (714 residues; (Wilkins et al., 1999)) is about 146 Å, and the center-to-center distance calculated from the density number is 288 Å. Likewise, based on the length of the disordered RGG domain (174 residues), the calculated hydrodynamic diameter is 80 Å and the center-to-center distance calculated from the density number is 175 Å. In both cases, these figures suggest that LAF-1 molecules are far away from each other, separated by roughly 95–140 Å. Perplexingly, at the measured concentrations, the intermolecular contacts should be scarce and the magnitude of the attractive forces between molecules very weak. However, alternative explanations were proposed

for the unusually low concentration measured by usFCS in LAF-1 condensates (McCall et al., 2020).

Seeking an explanation for the low concentration in LAF-1 condensates, Wei et al. quantified the magnitude of the forces between LAF-1 molecules by measuring the diffusion coefficient as a function of protein and salt concentration, which allowed extracting second virial coefficients, B_2. The results indicated that below 1 M NaCl and at protein concentrations lower than that of the dilute phase, these forces were strongly self-associative, and this result was corroborated by right-angle light scattering experiments. Therefore, separation of LAF-1 condensed phase could take place despite its low concentration. Additionally, measured B_2 values for the RGG domain in isolation evidenced attractive intermolecular forces even stronger than those for the complete LAF-1 protein, which is consistent with RGG being a highly 'sticky' domain that drives phase separation.

The relationship between spatial separation and associative forces in LAF-1 RGG molecules was further considered by Wei et al. using molecular simulations. By calculating the pervaded volume associated to each protein chain, they found that the RGG domains underwent large-scale conformational fluctuations, encompassing globular conformations and expanded coil-like states sampled with roughly equivalent probabilities. The expanded conformations of up to 140 Å hydrodynamic diameter generate large pervaded volumes, which increases the likelihood that RGG domains transiently contact and overlap each others, despite their low concentration. Furthermore, Wei et al. assessed the nanorheology of LAF-1 and found that the mesh formed by condensation had an effective size of 30–80 Å. An effective mesh of this size is consistent with the molecular shape and intermolecular distances calculated above and reveals the void-rich nature of LAF-1 droplets. Most importantly, condensates with this mesh size could serve as selective filters for macromolecules *in vivo*.

4.3.9. Elastomeric proteins

Elastomeric peptides and proteins are molecules with growing importance in biology and in the development of biomaterials. The elastin monomer, tropoelastin, undergoes a well-characterized lower-critical-solution temperature phase separation (Muiznieks et al., 2018). Tropoelastin possesses alternating hydrophobic domains (HDs) and cross-linking domains (CLDs). HDs are disordered domains required for liquid-phase separation, which are composed of pseudo repetitive sequence motifs enriched in glycine, proline, and hydrophobic amino acids. CLDs are structural domains implicated in the covalent cross-linking of lysine residues. Elastin-like polypeptides (ELPs) derived from elastin are suitable models to study liquid-phase separation and chemical polymerization (Uversky, 2017). Typically, ELPs contain repetitive CLDs and HDs representative of those observed in tropoelastin sequences.

Reichheld et al. used NMR spectroscopy to study the structure and dynamics of a designed ELP, ELP3, through liquid-phase separation and formation of a cross-linked elastic material (Reichheld et al., 2017). After inducing phase separation by raising the temperature, the $^{1}H–^{15}N$ HSQC spectrum showed two overlapping sets of resonances, which were identified as arising from the dilute and dense phase, respectively. Nearly complete backbone resonance assignment for ELP3 prior and after phase separation indicated that ELP3 was highly disordered in both the dilute and phase-separated state. Moreover, backbone and side chain chemical shifts were essentially identical in both phases, strongly suggesting that no substantial conformation changes occurred during condensation. NMR also showed that CLDs displayed very low α-helical propensity, whereas HDs had partial β-strand structure. However, the most interesting finding in this study is that strong NOEs from multiple, nonspecific, intermolecular hydrophobic contacts from side chain resonances of alanine, valine, and proline residues were detected only in the condensate, because in the dilute phase hydrophobic contact NOEs were mainly intramolecular. This differential behavior suggests that HDs are the main responsible factor driving liquid condensation.

Comparing the diffusion rate of ELP3 within the dilute phase with that of the condensed phase, Reichheld et al. were able to estimate that protein concentration in the condensate was 42 mM ($\Phi_D = 0.42$). Using *Eqn. (5)*, the number density in the protein-rich phase, and the unfolded diameter of the molecule (estimated from the number of residues), we calculate that the overlapping volume per interaction is 33%. Thus, with this degree of molecular overlapping, the number of intermolecular interactions should be very large.

In a clever approach, as a model system of liquid phase separation, Simon et al. used a microfluidic generator to create uniform, roughly cell-sized aqueous microdrops immersed in oil (Simon et al., 2017). With their device, phase separation of engineered ELPs within the microdrops was triggered by temperature changes to generate a range of condensates structures with controllable architecture, size and composition. A relevant example in the study was an 80-residue-long ELP, E3, for which a complete phase diagram was determined. Based on the right arm of the diagram, E3 liquid condensate is 11 mM ($\Phi_D = 0.37$). The number density along with the estimated disordered diameter of E3 allow to apply *Eqn. (5)* to conclude that the overlapping volume per interaction is 34%. As above, with this degree of molecular overlapping, intermolecular interactions would be extensive.

4.4. Mesoscopic clusters

Although nanoscale condensation of protein chains in homogeneous solutions had long been suspected, only recently its significance was convincingly demonstrated, both *in vitro* and *in vivo*. (Georgalis et al., 1999; Gliko et al., 2005; Pan et al., 2010; Chan et al., 2012; Maes et al., 2015; Safari et al., 2015; Keber et al., 2021; Alberti and Hyman, 2021). These condensates —named mesoscopic clusters, nanocondensates, and nanoscale clusters— are metastable anomalous condensates of 10^4–10^6 molecules and sizes under a few hundred manometers.

Mesoscopic clusters are deemed important precursors in nucleation processes, such as crystallization, irreversible aggregation, and fibrillation; in turn, these nucleation processes characterize many physiological and pathological conditions (Vekilov, 2004; Pan et al., 2010; Sleutel and Van Driessche, 2014; Sosa et al., 2016; Schubert et al., 2017; Chan and Lubchenko, 2019; Toledo et al., 2019; Choi et al., 2020; Xu et al., 2021; Yang et al., 2021; Petronilho et al., 2021; Parchure et al., 2021). In addition to proteins, amphiphilic amino acids and small organic compounds were shown to form mesoscopic clusters (Warzecha et al., 2017; Yuan et al., 2019).

The physicochemistry of mesoscopic condensation in liquid solutions is far from being well understood, and its emerging features are surprising. Mesoscopic aggregates are distinct from conventional condensates produced by liquid-liquid phase separation (Safari et al., 2017). First, although the clusters are likely of a liquid nature, they exist under conditions where macroscopic protein dense liquids do not. Second, in mesoscopic clusters the concentration of the dilute phase increases as the total concentration of the system increases, whereas in normal liquid condensates it remains relatively constant and independent of the total concentration. Third, the size of a mesoscopic clusters is narrowly distributed around a steady-state value and independent of the total concentration, whereas in normal liquid condensates it is much more variable and dependent of the total concentration. Fourth, the volume fraction of the mesoscopic aggregate depends only on the number of mesoscopic clusters, whereas in normal liquid condensates it depends on both the number and the size (Pan et al., 2010). The above features also distinguish mesoscopic clusters from other common protein condensates such as crystals, amyloid fibrils, gels, and amorphous precipitates (Safari et al., 2019; Yang et al., 2021). Accordingly, different mechanisms for reversible mesoscopic aggregation have been proposed (Safari et al., 2017; Chan and Lubchenko, 2019).

Mesoscopic clusters of several different proteins has been characterized: hemoglobin, lysozyme lumazine synthase, glucose isomerase, and huntingtin (Georgalis et al., 1999; Galkin et al., 2007; Gliko et al., 2007;

Knee and Mukerji, 2009; Pan et al., 2010; Li et al., 2011; Li et al., 2012; Sleutel and Van Driessche, 2014; Maes et al., 2015; Safari et al., 2015; Maes et al., 2015; Safari et al., 2017; Van Posey et al., 2018; Nikfarjam et al., 2019).

A single point mutation in hemoglobin (Hb) causes sickle cell disease, in which mutant Hb (HbS) forms long pathological fibers in a temperature dependent manner. In concentrated solutions, the nucleation of HbS polymers is preceded by the formation of metastable clusters (Pan et al., 2007; Knee and Mukerji, 2009). Dynamic light scattering (DLS) showed that typical mesoscopic clusters of deoxy HbS, oxy HbA, and oxy HbS were 600, 750, and 1000 nm in diameter, respectively.

In 1999, using DLS and static light scattering (SLS), Georgalis et al. reported clusters of 200–400 nm in diameter in lysozyme solutions, (Georgalis et al., 1999), and in 2010, using the same experimental approach, Pan et al. observed steady lysozyme clusters of 100 nm (Pan et al., 2010). After a thorough theoretical, thermodynamic, and kinetic analysis these authors postulated that protein mesoscopic clusters were non-equilibrium, long-lived, liquid conglomerates of protein molecules and transient protein complexes. Subsequent work using DLS, SLS and Brownian microscopy confirmed that lysozyme populates clusters of about 100 nm in diameter (Li et al., 2011; Y. Li et al., 2012; Safari et al., 2015; Safari et al., 2017). Furthermore, it was concluded that (a) the cluster size increased slowly with time but was independent of lysozyme concentration, (b) the change in size did not constitute a slow evolution to a stable macroscopic phase, and (c) lysozyme clusters were in equilibrium with the solution, and their formation was a reversible process (Y. Li et al., 2012). More recently, the notion that lysozyme mesoscopic clusters are in equilibrium with protein monomers was challenged by systematic filtering the assayed solutions. In agreement with the previous works, 30- and 100-nm clusters were observed in samples filtered through filters with 100-nm pores. However, filtration through 20-nm pores totally removed the clusters, and they did not reappear with time, even at high temperatures or in denaturing conditions, as they would if they were equilibrium species (Nikfarjam et al., 2019).

Mesoscopic clusters of glucose isomerase were studied by Sleutel et al. (Sleutel and Van Driessche, 2014). Using Brownian microscopy, they found clusters of 300 nm in diameter that were stable in time. Furthermore, these clusters were in equilibrium with the bulk solution and participated in crystal growth. However, cluster reappearance from cluster-free solutions was appreciably slower than cluster dissolution, and no detectable cluster formation was detected below a critical protein bulk concentration. In another study, aged solutions of glucose isomerase containing clusters of 500–1000 nm were analyzed by DLS, confocal depolarized DLS, and oblique illumination dark-field microscopy. The results suggested that the mesoscopic clusters of glucose isomerase were liquid or amorphous solids and could locate crystal formation (Maes et al., 2015).

The lumazine synthase/riboflavin synthase complex, which catalyzes the synthesis of riboflavin, comprises a homotrimer, corresponding to riboflavin synthase and a 60-mer, corresponding to lumazine synthase (Ladenstein et al., 2013). However, under certain conditions, lumazine synthase itself forms a hollow, homo 60-mer of about 1000 kDa and 16 nm in diameter. This lumazime particle was studied by DLS and found to populate a mesoscopic aggregate of about 350 nm (Gliko et al., 2007). Based on the mass of a single particle and an estimate of cluster density, we calculate that each mesoscopic aggregate contain 10^3 60-mers.

Huntington's disease, a disorder that affects neurons, is characterized by the deposit of insoluble aggregates of the N-terminal region of a pathological variant of huntingtin (Htt). The pathological variant includes in the N-terminus a polyglutamine track (polyQ) much longer than normal, and this polyQ expansion causes a toxic gain of function (Walker, 2007). A phase diagram with at least three distinct phases was proposed for a 78-residue, N-terminal segment of huntingtin including a 40-residue polyQ repeat (Posey et al., 2018). In equilibrated solutions, these phases were analyzed by electronic transmission microscopy (ETM). According to the images, one of the two soluble phases comprised mainly monomers and oligomers, and the other was enriched in mesoscopic clusters of 25 nm in diameter —it can be estimated that aggregates of 25 nm would contain about 500 molecules. The third phase was fibrillar. However, the only technique employed to measure the aggregates was ETM, and it would be desirable to confirm the above findings with complementary DLS and Brownian microscopy measurements.

The tumor suppressor p53 is a transcription factor whose inactivation is related to almost every cancer, either through mutations in the TP53 gene or deregulation of its associated pathways (Levine, 2019). Numerous mutations that destabilize p53 and promote its aggregation and fibrillation have been characterized, and p53 R248Q is one of the most commonly found in breast cancers. The phase behavior of p53 was thoroughly examined by the group of Peter Vekilov (Safari et al., 2019; Yang et al., 2021). In cellular studies, they combined staining with an antibody specific for misfolded or aggregated p53, an antibody directed against the N-terminal transactivation domain of p53, and the amyloid probe Thioflavin T. All together, the results suggested that p53 R248Q forms aggregates with narrow size distribution within the cytoplasm of breast cancer cells, whereas wild-type p53 does not. These p53 R248Q aggregates were visualized as *puncta* with 0.6–1.0 μm in diameter and exhibited a behavior incompatible with fibrils or droplets of stable dense liquid.

In dilute solutions, purified p53 also formed aggregates that could be monitored by oblique illumination microscopy (OIM) and DLS. OIM is a technique that tracks Brownian movements of particles and measures diffusion coefficients from trajectories. Particle sizes were extracted from the diffusion coefficients using the Einstein-Stokes relation (Li et al., 2011; Vorontsova et al., 2016). At 15 °C, 220-nm filtered p53 solutions produced no OIM-traceable speckles after 20 min observations, and particle sizes measured by DLS indicated radii of 6 nm corresponding to p53 tetramers and low order oligomers. At 25 °C, mesoscopic aggregates of ca. 50 nm radii were detected by OIM. Increasing temperature resulted in particles with increased radii, and at 37 °C these reached 145 nm. Interestingly, particle density number also increased with temperature. DLS measurements at 37 °C confirmed the presence of particles of 145 nm coexisting with the 6-nm p53 tetramer. In addition, DLS showed that the volume fraction of the aggregate increased with the initial p53 concentration, whereas the size of the individual particles remained constant. This behavior of p53 mesoscopic aggregates is in striking contrast with normal liquid-liquid phase separation, because in the latter, as the mixed solution concentration increases, one sees a constant concentration of the bathing solution and an increase of particle volume.

As mentioned above, p53 mutant R248Q exhibited an enhanced tendency to form mesoscopic clusters; whereas wild-type p53 exhibited no clusters at 15 °C, R248Q p53 formed aggregates of 50 nm radii on average. Our calculations show that mesoscopic clusters of this size could contain 10^3 loosely packed p53 tetramers each.

In Vekilov's works, a model based on the p53 results was proposed to explain the differences between mesoscopic clusters and normal liquid condensation. In this model, clusters form because of the accumulation of transient misassembled oligomers. In turn, misassembly is promoted by conformational destabilization, and cluster's growth in size and number with temperature is related to the unfolding of p53. Likely, mesoscopic clusters of p53 are transient formations in route to normal liquid condensation, gelation, fibrillation, and amorphous precipitation. In this regard, p53 mutants form classical liquid droplets that turn more rapidly into solid-like aggregates compared with the wild-type protein (Pedrote et al., 2020; Petronilho et al., 2021).

5. Promising trends in biomolecular condensation

5.1. Regulation of condensate properties and dynamic

Depending on the biological function cellular condensates can contain hundreds or even thousands of different proteins and nucleic acids (Feng et al., 2021; Orti et al., 2021; Alberti and Hyman, 2021).

Some components are constitutively retained and others are transiently recruited, and whereas some components are shared between different condensates others are specific to particular condensates. This poses the question as to how inclusion and exclusion are regulated. A simplified model posits that condensates include 'scaffold' and 'client' components (Banani et al., 2016, 2017) (Ditlev et al., 2018; Alberti and Hyman, 2021; Parchure et al., 2021). In this useful model, scaffold proteins are essential for the formation of condensates; clients are not required but interact selectively with scaffold proteins.

In the scaffold-client model, liquid phase separation occurs through the formation of dense networks of intermolecular interactions, in which the multivalency of each constituent is provided by folded domains and/or by IDDs (P. Li et al., 2012; Shin and Brangwynne, 2017; Kamagata et al., 2021; Mohanty et al., 2022; Feng et al., 2021). Interactions between folded domains are specific and stoichiometrically defined. Contrastingly, disordered domains harbor multiple, weak, unspecific (promiscuous) binding sites —also called 'stickers'— separated by 'spacers' regions along the sequence. Selection and enrichment of clients in condensates can be achieved by specific binding or by promiscuous affinity. The first usually involves folded domains, and the second is usually mediated by highly dynamic and fuzzy interactions of IDDs. We refer the reader to Feng et al. (2021) for further review on these two types of interactions.

When the interactions are very weak, the distinction between scaffolds and clients is difficult, and concerted participation of client-specific interactions is required for condensation. Given the central role attributed to scaffold proteins, the focus of much of the current research is on their role in the control of phase separation and the material properties of the condensates. Apparently, the concentration of client proteins in the condensates is related to the strength and specificity of the interactions with the scaffold. Strong specific interactions increase the concentration of client components up to 10,000-fold, as observed in chromatin condensates (Gibson et al., 2019). With weak unspecific interactions, such as those in IDD-driven phase separation, enrichment of client species is much less significant.

Cells can regulate phase separation by post-translational modifications, binding, conformational transitions, and environmental changes. However, these mechanisms frequently act in concert and are hard to dissect.

Regulation of phase separation by post-translational modifications takes place by creation or elimination of binding sites or motifs, as well as by modulation of the strength and specificity of the interactions (Nott et al., 2015; Banani et al., 2016; Alberti and Hyman, 2021). A prominent example is the phosphorylation and methylation, which increase the saturation concentration of FUS and change the material properties of its condensates (Monahan et al., 2017; Hofweber et al., 2018; Qamar et al., 2018). Other examples are the activation of the T cell receptor phosphorylation of signaling components on the plasma membrane (Su et al., 2016), the dissolution of several condensates during mitosis by the activity of the tyrosine-phosphorylation-regulated kinase 3 (Rai et al., 2018), and the fine-tuning of condensation or aggregation of a PLD and granulin fragments by the redox state of cysteine residues (Bhopatkar et al., 2022).

Binding of ligands regulates condensation by changing the behavior of phase separating proteins (Qamar et al., 2018; Guo et al., 2018; Hofweber et al., 2018; Yoshizawa et al., 2020; Sanders et al., 2020). The expression of ligands can be used to modify the saturation concentration of the scaffold and change accordingly the volume fraction of the condensate. This mode of regulation is called polyphasic linkage and is likely to occur widely in cells (Banerjee et al., 2017; Maharana et al., 2018; Ruff et al., 2021; Feng et al., 2021).

Conformational transitions regulate phase separation by changing the intermolecular affinity of condensing proteins. Reconstitution experiments showed that SGs are formed by RNA-mediated condensation of the RBP G3BP1. Under non-stress conditions, G3BP1 adopts an autoinhibitory compact conformation stabilized by electrostatic interactions between its RG-rich and disordered acidic regions. RNA competes with these interactions liberating the RG-rich region and promotes the formation of G3BP1 clusters. In turn, these clusters crosslink RNA molecules to form networks of G3BP1–RNA condensates which recruit other RBPs known to localize to SGs (Qamar et al., 2018; Guillén-Boixet et al., 2020; Yang et al., 2020; Alberti and Hyman, 2021).

Another example of conformational regulation is that of SOD1, a Zn-stabilized metalloenzyme associated with SGs. The presence of SGs comprising SOD1, TDP-43, and FUS is the pathogenic hallmark of ALS, and immature, intrinsically disordered apoSOD1 is presumably involved in the aggregation and recruitment into SGs. Folding of SOD1 is complex and involves copper and zinc metallation and disulfide bond formation. Whereas the disulfide reduced, fully metallated SOD1 does not undergo condensation, the metal-free apo variant forms liquid droplets that can be reversed by Zn addition. Furthermore, condensed apoSOD1 undergoes aggregation that cannot be reversed by Zn. ALS mutants with destabilized Zn binding sites also conform to the condensation-aggregation path and Zn susceptibility. Biophysical evidence demonstrates that the phase behavior is regulated by the conformational transition between a disordered and a relatively compact folded state of SOD1, providing a mechanisms for the cellular regulation of normal and pathological condensation and aggregation (Das et al., 2022).

Molecular chaperones and protein degradation systems constituting the protein quality control (PQC) machinery play a central role regulating the dynamic of condensates. The role of PQC in protein folding is well known; however, its participation in controlling the integrity and evolution of condensates is much less understood and the focus of intense scrutiny. Indeed, condensates are an integral part of PQC, since liquid phase separation allows its spatiotemporal regulation (Forman-Kay et al., 2018; Lei et al., 2021; Alberti and Hyman, 2021; Koopman et al., 2022).

Environmental changes resulting from stress, starvation, hypoxia, and metabolism have a profound effect on the constitution and dynamic of protein condensates. A few representative examples from the recent literature are presented next, focusing in the molecular mechanisms underlying the regulation of condensates.

Poly(A) binding protein 1 (Pab1), which plays key roles in mRNA polyadenylation, is a general marker of SGs that condensates *in vitro* upon exposure to heat and pH within biologically relevant ranges. The phase separation properties of Pab1 strongly depend on temperature and pH, making it a suitable stress sensor in cells. Accordingly, Pab1 LCD variants with altered thermal and pH-dependent condensation *in vitro* and *in vivo* compromised yeast growth during thermal and energy depletion stress (Riback et al., 2017).

ATP enhances LLPS of FUS at low concentration but dissolves condensates at high concentration. A similar effect of nucleic acids, including RNA and single-stranded DNA (ssDNA), has been observed for several RBPs, including FUS and TDP-43. Since ATP concentration in the cell is much higher than that needed for providing energy or for phosphorylation reactions, it is likely that the high concentration effect upon condensation results from its chaotropic nature (Kang et al., 2018; Maharana et al., 2018; Wang et al., 2018).

Pbp1, the yeast ortholog of ataxin-2 regulates several cellular processes. The LCD of Pbp1 forms labile aggregates that promote liquid-like or gel-like condensation. Unlike many other LCDs that are rich in phenylalanine or tyrosine residues, the Pbp1 LCD is rich in methionine residues, which are susceptible to oxidation by reactive oxygen species. This property allows the regulation of Pbp1 condensation by the redox state of the environment, and methionine oxidation disrupts Pbp1 liquid-like droplets reversibly by methionine sulfoxide reductase (Kato et al., 2019).

ERF-3 is a multidomain protein that includes a PLD, a disordered stress-sensor domain, and a folded catalytic domain. During cell growth, ERF-3 catalyzes termination of translation; under stress, the sensor domain, in concert with the PLD, promotes phase separation into condensates. A cluster of negatively charged amino acids in the stress-sensor domain senses pH and regulates condensate formation. Interestingly, the

isolated catalytic domain forms *in vitro* irreversible aggregates at all tested pHs, but the presence of the sensor domain restores the pH sensitivity of condensation and strongly inhibits irreversible aggregation. Thus, it was proposed that ERF-3 is a molecular device that sense and respond to environmental changes by modulating the fate and material properties of the condensates (Franzmann et al., 2018).

5.2. Conformational evolution of biomolecular condensates

Although at short-time scale liquid condensates can be regarded as reversible and stable states, they are actually metastable and can evolve, more or less rapidly, to different, less dynamics (more solid-like), physical states. This process is frequently referred to as aging, hardening, or maturation (Jawerth et al., 2020). The evolution of the material properties of the condensates is a hot topic in cell biophysics and physiology. Aging can involve distinct types of transitions. Transitions to gel-like states are brought about by the entanglement of the constituents and results in relatively static networks of interactions that extends through the whole phase. Transitions to solid-like phases can result in the formation of fibers, amyloids, crystal-like aggregates, or amorphous materials (Alberti and Hyman, 2021; Ray et al., 2021; Abyzov et al., 2022).

An illustrative example of the processes that liquid condensates can undergo is that of FUS, which is representative of many proteins associated with neurodegenerative diseases. Within hours, *in vitro* liquid condensates of FUS-LCD transition into a gel-like state, and this conversion is potentiated by disease-associated mutations. At longer times, FUS gel evolves into a fibrillar, amyloid-like material, and this fibrillation is faster for the mutants (Patel et al., 2015; Murakami et al., 2015; Murray et al., 2017). There is a general belief that the transformation of liquid condensates into pathological fibers and aggregates is of major significance in the development of ALS, other neurodegenerative diseases, and in aging. In this regard, the fibers and aggregates either could be toxic *per se* or their constituent proteins could be disabled for a physiological function (Murakami et al., 2015; Mackenzie et al., 2017; Wang et al., 2018; Murthy et al., 2019).

X-ray diffraction and electron microscopy data showed that FUS fibrillar material includes cross-β structure similar to that of pathogenic amyloid and prion fibrils (Kato et al., 2012). For its part, NMR study showed that a specific 57-residue segment in the N-terminal half of FUS-LCD forms the cross-β-fibril core, while the C-terminal FUS-LCD is disordered (Murray et al., 2017). However, unlike pathogenic fibrils, FUS fibrils were readily disassembled by mild treatments, which suggests that they are different from typical prion-like, irreversible fibers (Kato et al., 2012; Murakami et al., 2015; Lin et al., 2016).

Unexpectedly, cryogenic electron microscopy revealed that the C-terminal half of FUS-LCD —which, as mentioned above, is disordered in the structure of the full-length FUS-LC— also forms amyloid-like fibers with distinct conformation and symmetry. This important result underscores the diversity of structural motifs that FUS fibrils can adopt and fuels the quest for a fundamental understanding of fibril formation and of the variety of structures and sequences involved in physiological and pathological solid-like phases. Further, a deeper understanding of how protein deposits are formed and dissolved, and how they are related to cellular function and death, is eagerly awaited to develop therapeutic strategies for devastating degenerative diseases (Yuan et al., 2019; Lee et al., 2020; Mathieu et al., 2020; Chatterjee et al., 2022).

5.3. Biological function of condensates

As it became clear that condensates are directly or indirectly implicated in most cellular processes, the necessity arose of systematizing their functions and mechanisms of action. Whereas in the past the biological function of a condensate was a matter of empirical discovery, today it is assumed that any complex biological function is somehow related to a protein condensation. This tenet greatly accelerates the pace of discovery and fruitfully guides current experimental work. In this spirit, condensates were thoroughly classified by Michael K. Rosen group in functional classes organized and distance scales on which they operate (Lyon et al., 2021). In addition, the complex effects of phase separation on reaction rates and regulations of biochemical processes in eukaryotic cells were recently reviewed (Banani et al., 2017; Shin and Brangwynne, 2017; Mathieu et al., 2020).

Localization and concentration of the condensate's constituents modulate selectivity and reactivity, respectively. Selectivity is based in the porous nature and excluded volume effects of the condensates, which act like dynamic noncovalently crosslinked meshes of homo and heterotypic interactions. Reactivity is mainly based in the law of mass action, although molecular conformation, scaffold-induced molecular organizations, and changes in diffusion rates also modify reactivity (André and Spruijt, 2020; Ura et al., 2020; Peeples and Rosen, 2021; Zhang et al., 2021).

The prototypical example of increased reactivity and selectivity promoted by co-concentration of enzymes and substrates is the acceleration of the rate-limiting step in the photo-synthetic carboxylation of ribulose–bisphosphate by the enzyme Rubisco. Condensation enhances simultaneously the reaction rate and specificity by means of reactant's concentration and preferential concentration of CO_2 over competing oxygen. CO_2 and Rubisco concentrating mechanism in eukaryotic microalgae involves sequestration of the enzyme in the pyrenoid, a membraneless condensate in the chloroplast stroma. In bacteria, the concentration involves membraneless carboxysomes (Wunder et al., 2018; Flecken et al., 2020; Azaldegui et al., 2021; Wang et al., 2019; Zang et al., 2021).

Another outstanding case of co-concentration of enzymes and substrates is the production of purine to maintain cellular homeostasis and promote cell growth. Two complementary pathways act in concert to that end: the purine salvage and the *de novo* purine biosynthetic pathways. The last is activated when purine demand is high and converts phosphoribosyl pyrophosphate into inosine 5-monophosphate. In humans, this process consists of ten concerted reactions catalyzed by six enzymes and takes place in biomolecular condensates called purinosomes. In addition to the six main enzymes, purinosomes include downstream enzymes and regulatory proteins such as molecular chaperones and kinases. The whole is increasingly regarded as a *metabolon*, a highly complex network of enzymes aimed to channel metabolites through a given pathway. Investigation of such complex systems is just starting and promises to further our understanding of cell biophysics and biochemistry (Pedley et al., 2022).

Although in dense phases reaction rates are expected to increase, the actual effects can be quite variable. Reaction rates depend on multiple factors that, in some cases, can not be optimized by simply varying reactant's concentration. This happens because affinity and specific activity may not change concertedly to improve reactivity, and the increase in viscosity brought about by concentration may affect the diffusion of substrates and slow down reactions. Moreover, allosteric regulation may be hampered in crowded environments, and in consequence enzymatic activity may be affected (Nakashima et al., 2019; Peeples and Rosen, 2021). Also, congregating the multiple enzymes of a pathway increases the efficiency of the reactions by reducing the diffusion time of the intermediate products between sequential active sites. Similarly, the concentration of enzymes and substrates at one location (sequestration) may lead to their depletion at another, which may inhibit specific biochemical pathways. The complex effects of location and concentration on biological activity are further illustrated by the concentration of antineoplastic drugs in specific protein condensates and by the selective partitioning and concentration within condensates that contribute to drug pharmacodynamics (Klein et al., 2020).

Other molecular-scale functional aspects of protein condensates that are under intense scrutiny relate to proteostasis: protein biogenesis, folding, degradation, and trafficking. The function of condensates on protein synthesis is being investigated at accelerated pace, as evidenced by the numerous studies addressing nucleic acid–protein condensation, some of which were reviewed in preceding sections.

Two illustrative instances of the role of condensates in protein folding are those of nucleophosmin (NPM1) and heat-shock factor 1 (HSF1). NPM1 acts in the nucleus as a chaperone to prevent irreversible aggregation of misfolded proteins (Frottin et al., 2019). HSF1 promotes chaperone expression, increasing protein-folding capacity, improving protein homeostasis and cell survival. However, under stress, HSF1 also condensates in nuclear stress bodies whose dissolution, rather than formation, prompts HSF1 activity and cell survival. Moreover, during prolonged stress, HSF1 *foci* change from fluid into gel-like condensates, and cells concomitantly reduce gen induction and become apoptosis prone (Gaglia et al., 2020).

Compelling examples of the ongoing research on protein trafficking are recent works suggesting that proinsulin is organized in dynamic liquid-condensates at the trans-Golgi network (TGN) and that liquid-liquid phase separation facilitates protein sorting and packing into secretory granules (Kienzle and von Blume, 2014). Liquid chromogranin condensates recruit and sort proinsulin and other granule-destined cargo molecules towards secretory granules (Parchure et al., 2021).

The proteasome —a proteolytic machine for selective degradation of ubiquitylated proteins— mediates compartmentalized protein degradation in cytoplasm and nucleus, and it is associated with chromatin, cytoskeleton, and various membrane and membraneless condensates. Under stress conditions, when protein degradation is exacerbated, bodies and aggregates of the proteasome become prominent: the peri- or intranuclear quality control compartment JUNQ or INQ respectively, the cytosolic quality control-bodies (Q-bodies), stress foci, the peri-vacuolar Insoluble Protein Deposit (IPOD), and others (Kumar et al., 2017). The research on protein proteasomal degradation and quality control has been growing for decades and recently has acquired renewed impetus with the awareness on the importance of protein condensation in these cellular functions. For a recent review on this subject we refer the reader to the work of Xing Guo (2022). Finally, many examples of the various mechanisms through which condensation affects biological function at molecular scale were collected by Lyon et al. (2021).

Mesoscale functions are exercised by arrays of multiple coexisting condensates. Examples are the interconnection of biochemical processes, the arrangement of large intracellular structures, sensing, and force transduction.

Genomes undergo mesoscale changes that impact on protein expression and other cellular functions, and these changes can affect entire chromosomes, genomic regions, or local interactions between enhancers and promoters. All the levels of chromatin organization are influenced by interactions with proteins located in condensates and nuclear bodies (Pombo and Dillon, 2015; Shin and Brangwynne, 2017). Condensates participate in the formation of heterochromatin domains that are transcriptionally silent (Oh et al., 2022). They are also associated with active regions of lower chromatin density, euchromatin, as seen in the assembly of nucleoli at ribosomal DNA loci and in enhancer-rich gene clusters (Cho et al., 2018).

The production of ribosomes in the nucleolus is an outstanding example of mesoscale biochemistry. Preribosomal RNA is transcribed in the nucleolus innermost phase and is processed and assembled with ribosomal proteins in transit to the outer phases. Ribosome biogenesis reactions that take place in the nucleolus encompass five distinct processes: production of rRNAs by Pol I, pre-rRNA processing, pre-rRNA modification, assembly of precursor ribosomal subunits, and targeting of defective ribosomal subunit precursors for degradation. Further reading on nucleolar multiphase condensation and ribosome biogenesis can be found in an excellent review by Lafontaine et al. (2021).

The concerted action of multiple condensates has also been implicated in the transmission of epigenetic regulatory molecules or modifications, both the presynaptic active zone and the postsynaptic density, the DNA damage response, and the regulation of autophagy. For an enlightening review of these and other mesoscale functions we refer to Lyon et al. (2021).

5.4. Nanocondensates are ubiquitous

A significant proportion of cellular proteins dwells on the edge of solubility (Vecchi et al., 2020; Poudyal et al., 2022), and that might explain why nanocondensates (mesoscopic clusters) are ubiquitous. Historically, ideal protein solutions have been perceived as normal and aggregate states considered aberrant. However, our present perception of proteins is increasingly accepting aggregates and nanoclusters as normal inhabitants of the cell. Whereas the focus of most researches has been on large (>1 μm) condensates —easily accessible by conventional microscopy— many differential filtration and size exclusion studies suggested that the intact cytoplasm is organized into nanoassemblies (P. Li et al., 2012; Keber et al., 2021; Alberti and Hyman, 2021).

The molecular events underpinning the early stages of liquid condensate assembly and subsequent growth have just started to be elucidated. Classical nucleation theory predicts that proteins nucleate into stable assemblies directly in solution. Since direct nucleation may be quite slow, metastable liquid clusters may considerably accelerate further condensation and evolution to more ordered assemblies. This places mesoscopic clusters as obvious precursors in route to larger liquid condensates. Indeed, formation of mesoscopic clusters is a general phenomenon that can take place even for very small molecules such as amino acids (Rao and Parker, 2017; Liang et al., 2018; Yuan et al., 2019). However, the direct incorporation of monomers into nanocondensates and into growing liquid condensates warrants further investigation.

It is an exciting possibility that nanocondensates may have distinct biological roles. Following, we review a few outstanding examples that seems to indicate that indeed this is the case.

In a recent work, an impressive array of research groups reported that subsaturated solutions of RNA binding proteins from the FET family formed heterogeneous nanoclusters below saturating concentrations —below the concentrations at which macroscopic phase separation occurs (Kar et al., 2022). These authors suggest that cluster formation in subsaturated solutions and phase separation in supersaturated solutions are coupled through the strength of the interchain interactions, which warrants a flurry of research on the *in vivo* relevance and regulation of these clusters.

Nanoscale clusters of MEG-3 protein adsorb to the interface of *P* granules assembled by the proteins PGL-1 and PGL-3 and control their coarsening. Superresolution confocal microscopy confirmed that MEG-3 formed clusters of <160 nm at the PGL-3 interface *in vivo* and *in vitro* (*Folkmann* et al., *2021*). Interestingly, MEG-3 lowered the surface tension of PGL-3 condensates without changing their viscosity and established a physical barrier to their coalescence. As a result, surface adsorption of MEG-3 prevented coarsening without affecting PGL-3 exchange. In this regard, MEG-3 nanocondensates behave as Pickering agents, *i.e*, nanoscale particles that adsorb to interfaces and stabilize them (Yang et al., 2017). Importantly, these *in vitro* effects could be related to the *in vivo* phase behavior of *P* granules during oocyte maturation and polarization. Thus, nanocondensates acting as Pickering agents may be a general organizing principle for biomolecular condensates.

In living embryonic stem cells, Mediator and RNA polymerase II (Pol II) form small transient and large stable clusters (Cho et al., 2018); Mediator and Pol II co-localize in stable clusters that associate with chromatin, have material properties of phase-separated condensates, and respond to transcriptional inhibitors. Small, transient Mediator clusters are approximately 100 nm in size, whereas transient Pol II clusters appear somewhat larger. Mediator and Pol II co-condensate forming large (>300 nm) and more stable clusters. This suggests that large clusters of Mediator, transcription factors, and clustered enhancer elements interact with Pol II clusters in transcriptional condensates *in vivo*.

5.5. Molecular dynamics simulation of condensates

Nowadays, molecular dynamics (MD) is an essential tool to study structural and functional aspects of biomolecules, and the constant

growth in computational power dramatically expanded its use to study very large systems. Liquid-like condensates are very large systems, and the high resolution study of ordered-disordered domains in condensed states remains a daunting challenge. In this scenario, structural simulation emerges as a suitable, if not the only, tool to study submolecular details of self-assembly of large collection of molecules. Nevertheless, the number of molecules involved, even in a binary liquid condensate, is so large that precludes the description of the system with atomic details. To overcome this difficulty, coarse-grained MD techniques were developed, by which it is possible to construct phase diagrams for simulated systems and to characterize relevant biophysical parameters such as volume fractions, critical temperature, enthalpic and entropic contributions, and chain conformation (Hazra and Levy, 2021; Tesei et al., 2021). An additional complexity is that proteins involved in phase separation often contain multiple ordered and disordered domains, and therefore force fields must be accurate for both (Latham and Zhang, 2022).

An excellent example of coarse-grained MD study of liquid condensation is that of the tumor-suppressing protein p53. As mentioned in the preceding sections, p53 is a multifunctional transcription factor involved in a plethora of cellular functions, from DNA repair to apoptosis. The architecture of p53 is complex. It possesses trans-activation and proline-rich domains at the N-terminus, a structured DNA-binding domain at the core, and a tetramerization and a disordered domains at the C-terminus. *In vitro,* p53 forms liquid-like droplets via electrostatic interactions mediated by the high net charge of the N- and C-terminal unstructured domains (Kamagata et al., 2020). Recently, it was demonstrated that in the nucleus p53 undergoes a phase separation with liquid-like characteristics modulated by the trans-activation domain (Lemos et al., 2020; Petronilho et al., 2021). Moreover, Petronilho et al., observed a liquid-solid phase transition that could be attributed to the formation of amyloid oligomers (Petronilho et al., 2021).

In liquid droplets, p53 can act as a scaffold protein recruiting different kinds of client biomolecules. In coarse-grained MD simulations, p53 associates in a dense state akin to a liquid-like condensate. Interestingly, folded client domains diffuse into the condensates faster than the disordered ones, which is in agreement with microscopy experiments (Kamagata, 2021). As was found by Lemos et al., the diffusion process of guest proteins or ligands and the interaction with the host protein can alter or even dissolve the condensates (Lemos et al., 2020). The p53 case exemplifies the power of coarse-grained simulations to study the assembly of biomolecular condensates and predict the effect of temperature, osmolytes, guest proteins, ligand binding, and other factors.

5.6. The grammar of protein condensation

The relationship of sequence to protein condensation is the matter of intensive investigations. This is natural, because protein condensation is a collective protein folding process and, like unimolecular folding, is encoded in sequence space. The scope of these investigations is widely referred to as 'the grammar of protein condensation'. However, this catchy name should not obscure the important biophysical principles that it entails.

To unveil the relationship between sequence and phase separation, it was necessary first to develop dedicated databases to catalog and classify condensation-prone proteins. In recent years, we have seen the publication of several LLPS-specific databases, a comprehensive review of which is available (Pancsa et al., 2021). The more relevant databases are briefly described next.

LLPSDB v2.0 ((Wang et al., 2022); http://bio-comp.org.cn/llpsdbv2) has incorporated 586 independent proteins and 6678 specific conditions, including intrinsically disordered and folded domains as well as complexes between proteins and between proteins and nucleic acids. Given that this database only incorporates proteins associated with *in vitro* experimental data, the magnitude of its content reflects the extraordinary interest that protein condensation has aroused. Pha-SepDB2.0 ((You et al., 2020); http://db.phasep.pro/) contains 961 proteins with experimentally determined condensing properties and 6781 proteins associated to membraneless organelles. It was built based on UniProt localization annotations, literature searches and experimental data. DrLLPS ((Ning et al., 2020); http://llps.biocuckoo.cn), has collected condensing proteins using automated text mining procedures and classified them into scaffolds, regulators and clients. It contains reviewed, unreviewed and predicted entries. In addition, potential condensation-related proteins are identified through homology searches. PhaSePro ((Mészáros et al., 2020); https://phasepro.elte.hu) is a manually curated database of experimentally verified cases of LLPS. It has integrated biophysical biochemical and biological information. MLOs MetaDB ((Orti et al., 2021); http://mlos.leloir.org.ar/) has integrated the content of three different databases. It provides a consolidated and curated set of proteins and related biophysical processes, cellular localization, protein distribution across condensates and biological function.

Based in the large number of condensing proteins studied so far, a number of sequence-specific features that favor phase separation have been identified. These include electrostatic and polar interactions, π−π stacking and cation–π contacts, hydrophobic interactions, charge patterning, and low-complexity (Nott et al., 2015; Martin and Mittag, 2018; Vernon et al., 2018; Wang et al., 2018; Vernon and Forman-Kay, 2019; Gomes and Shorter, 2019; Martin et al., 2020; Dignon et al., 2020). It is worth noticing that, with the exception of low complexity, these sequence features are common in folded proteins. This is so because phase separation and folding are different aspects of the same fundamental biophysical process and therefore follow identical principles. Then, it is a legitimate question whether a grammar of protein condensation exists at all. The answer is found in the context in which phase separation occurs, one in which the intermolecular interactions prevail over the intramolecular ones. Any factor, extrinsic or intrinsic, that promotes intermolecular interactions favors collective condensation over intramolecular folding. All things considered, it seems better to speak of a grammar of condensation propensity, rather than a plain grammar of condensation. The list of condensation promoting factors is long and diverse, but those that stand out are bulk concentration and domain disorder. Concentration has to do with the solubility limit of the sequences and with cellular proteostasis; whereas domain disorder is encoded in sequence features, including low complexity and binding entropy, explaining why phase separation and domain disorder are intertwined.

Vernon et al. reviewed six sequence-based, first-generation methods developed to predict biologically relevant protein condensation (Vernon and Forman-Kay, 2019). The first, PLAAC ((Lancaster et al., 2014); http://plaac.wi.mit.edu/), was originally developed to detect prion-like sequences in the yeast proteome and turned to be effective in predicting other condensing proteins in different genomes. The second, LARKS (Hughes et al., 2021); https://srv.mbi.ucla.edu/LARKSdb/), exploits the fact that a large set of biological condensates contains low-complexity, aromatic-rich, kinked segments. In the third method, 'R + Y', by analyzing the FET family proteins, Wang et al. (2018) observed a correlation between the number of arginine and tyrosine residues and the critical concentration of condensation; extrapolating this correlation to non-FET proteins provided an estimate of the independent phase-separation propensity of a large percentage of the human proteome. The fourth method rests on the statistical frequency and sequence spacing of arginine and phenylalanine residues to identify DDX4-like sequences, and, since there is significant overlap between tyrosine-rich and phenylalanine-rich condensing sequences, it identifies both FET and DDX proteins (Nott et al., 2015). The fifth, the catGRANULE algorithm, was trained on the yeast proteome using sequence composition statistics and weighting residues by expected contribution to structural disorder, nucleic acid-binding propensity, sequence length, and the frequencies of arginine, glycine, and phenylalanine. Applied to proteomes, it gave a distribution of condensing scores (Bolognesi et al., 2016). The sixth of the predictors reviewed by Vernon et al. was PScore (Vernon et al., 2018). It uses sequence composition to estimate planar π-contact

rates of condensing proteins in comparison to structured proteins; the PScore planar π—π contacts are broadly associated with structural disorder, kinks in beta strands, nucleic acid binding, increased interactions with solvent, aromatic residues, and arginine.

More recently, improved first-generation condensation predictors have been developed. The PSPer method (Orlando et al., 2019); www.bio2byte.be/b2btools/psp/) implements a Hidden Markov Model with a probabilistic description of condensing sequences. It was trained against ordered proteins and might be biased toward disorder. GraPES, the prediction of biological condensate constituents server (Kuechler et al., 2022); https://grapes.msl.ubc.ca/), was originally meant to target SG constituents but showed predictive power also for those proteins that localize into other biological condensates.

All the above methods suffer limitations from the heterogeneous protein features on which they are based. More inclusive prediction tools, with general application, were needed, and in the last few years several methods were developed aiming to fulfill this need. Based in the observation that many proteins exhibit high conformational entropy upon binding and that conformational entropy can be predicted from sequence, Hardenberg et al. developed a method, the FuzPred method (http://protdyn-fuzpred.org) for predicting the binding modes of disordered proteins based on their amino acid sequences (Hardenberg et al., 2020; Miskei et al., 2020). Using this method, the authors identified proteins predicted to condense spontaneously under physiological conditions and estimated that they comprise about 40% of the human proteome. Importantly, they also predicted that most human proteins are potential clients in condensation processes. Saar et al. extracted biophysical and sequence-specific features of phase-separating proteins, combined them with neural network-based sequence embeddings, and trained machine-learning classifiers to identify condensing sequences with high accuracy (Saar et al., 2021). Their predictor, termed DeePhase, https://deephase.ch.cam.ac.uk/, distinguished condensing-prone sequences, for both structured and from unstructured proteins. PSPredictor is another sequence-based machine-learning condensation predictor based in LLPSDB. The PSPredictor's algorithm captures composition and sequence information identifying SGs scaffold proteins and predicting condensing candidates (Chu et al., 2022); http://www.pkumdl.cn/PSPredictor).

A fundamental difficulty that all condensation predictors face is the lack of a set of truly negative controls, since all protein can undergo condensation under appropriate conditions. Calibrating algorithms against proteins that do not liquid condensate under physiological conditions is insufficient, given the diversity of protein concentration, pH and other environmental parameters found in biological contexts. A symmetrical difficulty arises from training the prediction methods on proteins identified in liquid condensates, for liquid condensation is not always the end point of phase separation, and aggregation, fibrillation or even crystallization may arise from initial liquid condensation; thus, the universe of true positive chains may be much larger than that being considered.

Another major difficulty is that current methods for predicting protein condensation are very heterogeneous in terms of principles methodologies and targets. This makes very difficult to use them to obtain a binary, yes or not, answer to the question if a protein of interest is a condensing protein. To date, no systematic comparative study on the efficiency of the different methods is available; however, a judicious, combination of them seems very efficient for the identification of condensing proteins (Pancsa et al., 2021).

6. Concluding remarks

Biomolecular condensates are at the crossroad of two foundational concepts: cellular compartmentalization and protein conformation. Many decades of study of protein conformation have led to a new paradigm, in which the biological activity of proteins is not longer limited to an uniquely defined and ordered conformation and neither is tied to a single molecular structure. Concurrently, the study of membraneless subcellular compartmentalization has revealed that biomolecular condensates are large collections of protein molecules with extreme conformational diversity, and whose biological function is the spatiotemporal organization and regulation of biochemical reactions and cellular processes. This convergence of concepts allows to define two levels in the protein conformational landscape: intramolecular folding of isolated molecules and condensation folding (phase separation) of macromolecular ensembles.

Biomolecular condensation is driven by multivalent intermolecular interactions and mediated by order-disorder transitions of protein conformation and by protein domain architecture. The physicochemical forces and principles that govern protein condensation are the same that govern protein folding. However, what makes the difference is the high concentration of the intervening parties. Folding of diluted, undisturbed, foldable proteins leads spontaneously to ordered and unique tridimensional structures, whereas folding of concentrated and conformationally diverse protein chains in crowded and heterogeneous milieus leads to biomolecular condensates.

Biomolecular condensation and intramolecular folding are not mutually exclusive, and multidomain proteins with folded and disordered domains are conspicuous constituents of biomolecular condensates. This behavior is explained by the fact that both phenomena are encoded in protein sequence. What determine the fate of a particular sequence is the balance of intra and intermolecular interactions. Ultimately, all protein sequences, regardless their conformational status, will phase-separate with a variety of material properties if their solubility line in the phase diagram is crossed. The formation and regulation of functional biomolecular condensates is in the realm of cellular proteostasis and metabolism.

CRediT authorship contribution statement

Diego S. Vazquez: Writing – review & editing. **Pamela L. Toledo:** Writing – review & editing. **Alejo R. Gianotti:** Writing – review & editing. **Mario R. Ermácora:** Conceptualization, Writing – review & editing.

Declaration of competing interest

The authors declare the following financial interests/personal relationships which may be considered as potential competing interests: Mario R. Ermácora reports financial support was provided by National University of Quilmes. Conicet, and Agencia Nacional de Promoción Científica y Tecnológica, Argentina.

Data availability

Data will be made available on request.

Acknowledgments

This work was supported by grants from Universidad Nacional de Quilmes (PUNQ 53/1024), CONICET (PIP-GI 11220200101054CO), and Agencia Nacional de Promoción Científica y Tecnológica (PICT2016 0584), Argentina.

References

Aarum, J., Cabrera, C.P., Jones, T.A., Rajendran, S., Adiutori, R., Giovannoni, G., Barnes, M.R., Malaspina, A., Sheer, D., 2020. Enzymatic degradation of RNA causes widespread protein aggregation in cell and tissue lysates. EMBO Rep. 21, e49585.

Abyzov, A., Blackledge, M., Zweckstetter, M., 2022. Conformational dynamics of intrinsically disordered proteins regulate biomolecular condensate chemistry. Chem. Rev. 122, 6719–6748.

Adamcik, J., Mezzenga, R., 2018. Amyloid polymorphism in the protein folding and aggregation energy landscape. Angew. Chem. Int. Ed. 57, 8370–8382.

Alberti, S., Gladfelter, A., Mittag, T., 2019. Considerations and challenges in studying liquid-liquid phase separation and biomolecular condensates. Cell 176, 419–434.
Alberti, S., Hyman, A.A., 2021. Biomolecular condensates at the nexus of cellular stress, protein aggregation disease and ageing. Nat. Rev. Mol. Cell Biol. 22, 196–213.
André, A.A.M., Spruijt, E., 2020. Liquid–liquid phase separation in crowded environments. Int. J. Mol. Sci. 21, 5908.
Arakawa, T., Timasheff, S.N., 1985. Theory of protein solubility. In: Methods in Enzymology. Elsevier, pp. 49–77.
Astbury, W.T., Street, A., 1931. X-ray studies of the structure of hair, wool, and related fibres.-I. General. Philos. Trans. R. Soc. London, Ser. A 75–101.
Azaldegui, C.A., Vecchiarelli, A.G., Biteen, J.S., 2021. The emergence of phase separation as an organizing principle in bacteria. Biophys. J. 120, 1123–1138.
Banani, S.F., Rice, A.M., Peeples, W.B., Lin, Y., Jain, S., Parker, R., Rosen, M.K., 2016. Compositional control of phase-separated cellular bodies. Cell 166, 651–663.
Banani, S.F., Lee, H.O., Hyman, A.A., Rosen, M.K., 2017. Biomolecular condensates: organizers of cellular biochemistry. Nat. Rev. Mol. Cell Biol. 18, 285–298.
Banerjee, P.R., Milin, A.N., Moosa, M.M., Onuchic, P.L., Deniz, A.A., 2017. Reentrant phase transition drives dynamic substructure formation in ribonucleoprotein droplets. Angew. Chem. 129, 11512–11517.
Banjade, S., Rosen, M.K., 2014. Phase transitions of multivalent proteins can promote clustering of membrane receptors. Elife 3, e04123.
Berland, C.R., Thurston, G.M., Kondo, M., Broide, M.L., Pande, J., Ogun, O., Benedek, G.B., 1992. Solid-liquid phase boundaries of lens protein solutions. Proc. Natl. Acad. Sci. USA 89, 1214–1218.
Bernal, J.D., Crowfoot, D., 1934. X-ray photographs of crystalline pepsin. Nature 133, 794–795.
Berry, J., Brangwynne, C.P., Haataja, M., 2018. Physical principles of intracellular organization via active and passive phase transitions. Rep. Prog. Phys. 81, 46601.
Beutel, O., Maraspini, R., Pombo-Garcia, K., Martin-Lemaitre, C., Honigmann, A., 2019. Phase separation of zonula occludens proteins drives formation of tight junctions. Cell 179, 923–936.
Bhopatkar, A.A., Dhakal, S., Abernathy, H.G., Morgan, S.E., Rangachari, V., 2022. Charge and redox states modulate granulin-TDP-43 coacervation toward phase separation or aggregation. Biophys. J. 121, 2107–2126.
Biswas, S., Mukherjee, B., Chakrabarti, B., 2021. Thermodynamics of droplets undergoing liquid-liquid phase separation. bioRxiv. https://doi.org/10.1101/2021.04.01.438092.
Boeynaems, S., Alberti, S., Fawzi, N.L., Mittag, T., Polymenidou, M., Rousseau, F., Schymkowitz, J., Shorter, J., Wolozin, B., Van Den Bosch, L., others, 2018. Protein phase separation: a new phase in cell biology. Trends Cell Biol. 28, 420–435.
Boisvert, F.-M., van Koningsbruggen, S., Navascués, J., Lamond, A.I., 2007. The multifunctional nucleolus. Nat. Rev. Mol. Cell Biol. 8, 574–585.
Bolognesi, B., Lorenzo Gotor, N., Dhar, R., Cirillo, D., Baldrighi, M., Tartaglia, G.G., Lehner, B., 2016. A concentration-dependent liquid phase separation can cause toxicity upon increased protein expression. Cell Rep. 16, 222–231.
Botterbusch, S., Baumgart, T., 2021. Interactions between phase-separated liquids and membrane surfaces. Appl. Sci. 11.
Brady, J.P., Farber, P.J., Sekhar, A., Lin, Y.-H., Huang, R., Bah, A., Nott, T.J., Chan, H.S., Baldwin, A.J., Forman-Kay, J.D., others, 2017. Structural and hydrodynamic properties of an intrinsically disordered region of a germ cell-specific protein on phase separation. Proc. Natl. Acad. Sci. USA 114. E8194-E8203.
Brangwynne, C.P., Eckmann, C.R., Courson, D.S., Rybarska, A., Hoege, C., Gharakhani, J., Jülicher, F., Hyman, A.A., 2009. Germline P granules are liquid droplets that localize by controlled dissolution/condensation. Science 324, 1729–1732.
Brocca, S., Grandori, R., Longhi, S., Uversky, V., 2020. Liquid–liquid phase separation by intrinsically disordered protein regions of viruses: roles in viral life cycle and control of virus–host interactions. Int. J. Mol. Sci.
Broide, M.L., Berland, C.R., Pande, J., Ogun, O.O., Benedek, G.B., 1991. Binary-liquid phase separation of lens protein solutions. Proc. Natl. Acad. Sci. USA 88, 5660–5664.
Burke, K.A., Janke, A.M., Rhine, C.L., Fawzi, N.L., 2015. Residue-by-residue view of in vitro FUS granules that bind the C-terminal domain of RNA polymerase II. Mol. Cell 60, 231–241.
Cardinaux, F., Gibaud, T., Stradner, A., Schurtenberger, P., 2007. Interplay between spinodal decomposition and glass formation in proteins exhibiting short-range attractions. Phys. Rev. Lett. 99, 118301.
Celetti, G., Paci, G., Caria, J., VanDelinder, V., Bachand, G., Lemke, E.A., 2020. The liquid state of FG-nucleoporins mimics permeability barrier properties of nuclear pore complexes. J. Cell Biol. 219.
Chan, H.Y., Lankevich, V., Vekilov, P.G., Lubchenko, V., 2012. Anisotropy of the coulomb interaction between folded proteins: consequences for mesoscopic aggregation of lysozyme. Biophys. J. 102, 1934–1943.
Chan, H.Y., Lubchenko, V., 2019. A mechanism for reversible mesoscopic aggregation in liquid solutions. Nat. Commun. 10, 1–11.
Chattaraj, A., Blinov, M.L., Loew, L.M., 2021. The solubility product extends the buffering concept to heterotypic biomolecular condensates. Elife 10, e67176.
Chatterjee, S., Kan, Y., Brzezinski, M., Koynov, K., Regy, R.M., Murthy, A.C., Burke, K.A., Michels, J.J., Mittal, J., Fawzi, N.L., others, 2022. Reversible kinetic trapping of FUS biomolecular condensates. Adv. Sci. 9, 2104247.
Cho, W.-K., Spille, J.-H., Hecht, M., Lee, C., Li, C., Grube, V., Cisse, I.I., 2018. Mediator and RNA polymerase II clusters associate in transcription-dependent condensates. Science 361, 412–415.
Choi, J.-M., Holehouse, A.S., Pappu, R.V., 2020. Physical principles underlying the complex biology of intracellular phase transitions. Annu. Rev. Biophys. 49, 107–133.
Chong, P.A., Forman-Kay, J.D., 2016. Liquid–liquid phase separation in cellular signaling systems. Curr. Opin. Struct. Biol. 41, 180–186.
Chong, S., Mir, M., 2021. Towards decoding the sequence-based grammar governing the functions of intrinsically disordered protein regions. J. Mol. Biol. 433, 166724.
Chu, X., Sun, T., Li, Q., Xu, Y., Zhang, Z., Lai, L., Pei, J., 2022. Prediction of liquid-liquid phase separating proteins using machine learning. BMC Bioinf. 23, 1–13.
Correll, C.C., Bartek, J., Dundr, M., 2019. The nucleolus: a multiphase condensate balancing ribosome synthesis and translational capacity in health, aging and ribosomopathies. Cells 8, 869.
Curtis, R.A., Newman, J., Blanch, H.W., Prausnitz, J.M., 2001. McMillan–Mayer solution thermodynamics for a protein in a mixed solvent. Fluid Phase Equil. 192, 131–153.
Das, B., Roychowdhury, S., Mohanty, P., Rizuan, A., Mittal, J., Chattopadhyay, K., 2022. Zn-dependent structural transition of SOD1 modulates its ability to undergo liquid-liquid phase separation. bioRxiv. https://doi.org/10.1101/2022.02.20.481199.
Dignon, G.L., Best, R.B., Mittal, J., 2020. Biomolecular phase separation: from molecular driving forces to macroscopic properties. Annu. Rev. Phys. Chem. 71, 53–75.
Ditlev, J.A., 2021. Membrane-associated phase separation: organization and function emerge from a two-dimensional milieu. J. Mol. Cell Biol. 13, 319–324.
Ditlev, J.A., Case, L.B., Rosen, M.K., 2018. Who's in and who's out—compositional control of biomolecular condensates. J. Mol. Biol. 430, 4666–4684.
Dodson, G., Steiner, D., 1998. The role of assembly in insulin's biosynthesis. Curr. Opin. Struct. Biol. 8, 189–194.
Dumetz, A.C., Chockla, A.M., Kaler, E.W., Lenhoff, A.M., 2008. Protein phase behavior in aqueous solutions: crystallization, liquid-liquid phase separation, gels, and aggregates. Biophys. J. 94, 570–583.
Elbaum-Garfinkle, S., Kim, Y., Szczepaniak, K., Chen, C.C.-H., Eckmann, C.R., Myong, S., Brangwynne, C.P., 2015. The disordered P granule protein LAF-1 drives phase separation into droplets with tunable viscosity and dynamics. Proc. Natl. Acad. Sci. USA 112, 7189–7194.
Etibor, T.A., Yamauchi, Y., Amorim, M.J., 2021. Liquid biomolecular condensates and viral lifecycles: review and perspectives. Viruses 13, 366.
Feng, Z., Jia, B., Zhang, M., 2021. Liquid–liquid phase separation in biology: specific stoichiometric molecular interactions vs promiscuous interactions mediated by disordered sequences. Biochemistry 60, 2397–2406.
Flecken, M., Wang, H., Popilka, L., Hartl, F.U., Bracher, A., Hayer-Hartl, M., 2020. Dual functions of a rubisco activase in metabolic repair and recruitment to carboxysomes. Cell 183, 457–473.
Flory, P.J., 1942. Thermodynamics of high polymer solutions. J. Chem. Phys. 10, 51–61.
Folkmann, A.W., Putnam, A., Lee, C.F., Seydoux, G., 2021. Regulation of biomolecular condensates by interfacial protein clusters. Science 373, 1218–1224.
Fomicheva, A., Ross, E.D., 2021. From prions to stress granules: defining the compositional features of prion-like domains that promote different types of assemblies. Int. J. Mol. Sci. 22, 1251.
Forman-Kay, J.D., Kriwacki, R.W., Seydoux, G., 2018. Phase separation in biology and disease. J. Mol. Biol. 430, 4603.
Fox, A.H., Nakagawa, S., Hirose, T., Bond, C.S., 2018. Paraspeckles: where long noncoding RNA meets phase separation. Trends Biochem. Sci. 43, 124–135.
Franzmann, T.M., Jahnel, M., Pozniakovsky, A., Mahamid, J., Holehouse, A.S., Nüske, E., Richter, D., Baumeister, W., Grill, S.W., Pappu, R.V., others, 2018. Phase separation of a yeast prion protein promotes cellular fitness. Science 359, eaao5654.
Frey, S., Görlich, D., 2007. A saturated FG-repeat hydrogel can reproduce the permeability properties of nuclear pore complexes. Cell 130, 512–523.
Fritsch, A.W., Diaz-Delgadillo, A.F., Adame-Arana, O., Hoege, C., Mittasch, M., Kreysing, M., Leaver, M., Hyman, A.A., Jülicher, F., Weber, C.A., 2021. Local thermodynamics govern formation and dissolution of *Caenorhabditis* elegans P granule condensates. Proc. Natl. Acad. Sci. USA 118, e2102772118.
Frottin, F., Schueder, F., Tiwary, S., Gupta, R., Körner, R., Schlichthaerle, T., Cox, J., Jungmann, R., Hartl, F.U., Hipp, M.S., 2019. The nucleolus functions as a phase-separated protein quality control compartment. Science 365, 342–347.
Gaglia, G., Rashid, R., Yapp, C., Joshi, G.N., Li, C.G., Lindquist, S.L., Sarosiek, K.A., Whitesell, L., Sorger, P.K., Santagata, S., 2020. HSF1 phase transition mediates stress adaptation and cell fate decisions. Nat. Cell Biol. 22, 151–158.
Galkin, O., Pan, W., Filobelo, L., Hirsch, R.E., Nagel, R.L., Vekilov, P.G., 2007. Two-step mechanism of homogeneous nucleation of sickle cell hemoglobin polymers. Biophys. J. 93, 902–913.
Georgalis, Y., Umbach, P., Saenger, W., Ihmels, B., Soumpasis, D.M., 1999. Ordering of fractal clusters in crystallizing lysozyme solutions. J. Am. Chem. Soc. 121, 1627–1635.
Ghosh, B., Bose, R., Tang, T.Y.D., 2021. Can coacervation unify disparate hypotheses in the origin of cellular life? Curr. Opin. Colloid Interface Sci. 52, 101415.
Giannattasio, G., Zanini, A., Meldolesi, J., 1975. Molecular organization of rat prolactin granules: in vitro stability of intact and "membraneless" granules. J. Cell Biol. 64, 246–251.
Gibson, B.A., Doolittle, L.K., Schneider, M.W.G., Jensen, L.E., Gamarra, N., Henry, L., Gerlich, D.W., Redding, S., Rosen, M.K., 2019. Organization of chromatin by intrinsic and regulated phase separation. Cell 179, 470–484.
Gliko, O., Neumaier, N., Fischer, M., Haase, I., Bacher, A., Weinkauf, S., Vekilov, P.G., 2005. Dense liquid droplets as a step source for the crystallization of lumazine synthase. J. Cryst. Growth 275, e1409–e1416.
Gliko, O., Pan, W., Katsonis, P., Neumaier, N., Galkin, O., Weinkauf, S., Vekilov, P.G., 2007. Metastable liquid clusters in super-and undersaturated protein solutions. J. Phys. Chem. B 111, 3106–3114.
Goetz, S.K., Mahamid, J., 2020. Visualizing molecular architectures of cellular condensates: hints of complex coacervation scenarios. Dev. Cell 55, 97–107.
Gomes, E., Shorter, J., 2019. The molecular language of membraneless organelles. J. Biol. Chem. 294, 7115–7127.
Grouazel, S., Bonnete, F., Astier, J.-P., Ferte, N., Perez, J., Veesler, S., 2006. Exploring bovine pancreatic trypsin inhibitor phase transitions. J. Phys. Chem. B 110, 19664–19670.
Guillén-Boixet, J., Kopach, A., Holehouse, A.S., Wittmann, S., Jahnel, M., Schlüßler, R., Kim, K., Trussina, I.R.E.A., Wang, J., Mateju, D., others, 2020. RNA-induced

conformational switching and clustering of G3BP drive stress granule assembly by condensation. Cell 181, 346–361.
Guin, D., Gruebele, M., 2019. Weak chemical interactions that drive protein evolution: crowding, sticking, and quinary structure in folding and function. Chem. Rev. 119, 10691–10717.
Guo, L., Kim, H.J., Wang, H., Monaghan, J., Freyermuth, F., Sung, J.C., O'Donovan, K., Fare, C.M., Diaz, Z., Singh, N., others, 2018. Nuclear-import receptors reverse aberrant phase transitions of RNA-binding proteins with prion-like domains. Cell 173, 677–692.
Guo, X., 2022. Localized proteasomal degradation: from the nucleus to cell periphery. Biomolecules 12, 229.
Haas, C., Drenth, J., 1999. Understanding protein crystallization on the basis of the phase diagram. J. Cryst. Growth 196, 388–394.
Hardenberg, M., Horvath, A., Ambrus, V., Fuxreiter, M., Vendruscolo, M., 2020. Widespread occurrence of the droplet state of proteins in the human proteome. Proc. Natl. Acad. Sci. USA 117, 33254–33262.
Harpaz, Y., Gerstein, M., Chothia, C., 1994. Volume changes on protein folding. Structure 2, 641–649.
Hazra, M.K., Levy, Y., 2021. Biophysics of phase separation of disordered proteins is governed by balance between short-and long-range interactions. J. Phys. Chem. B 125, 2202–2211.
Hilser, V.J., Gómez, J., Freire, E., 1996. The enthalpy change in protein folding and binding: refinement of parameters for structure-based calculations. Proteins: Struct., Funct., Bioinf. 26, 123–133.
Hofweber, M., Hutten, S., Bourgeois, B., Spreitzer, E., Niedner-Boblenz, A., Schifferer, M., Ruepp, M.-D., Simons, M., Niessing, D., Madl, T., others, 2018. Phase separation of FUS is suppressed by its nuclear import receptor and arginine methylation. Cell 173, 706–719.
Holehouse, A.S., Pappu, R.V., 2018a. Collapse transitions of proteins and the interplay among backbone, sidechain, and solvent interactions. Annu. Rev. Biophys. 47, 19–39.
Holehouse, A.S., Pappu, R.V., 2018b. Functional implications of intracellular phase transitions. Biochemistry 57, 2415–2423.
Honda, K., Matsuyama, T., 1999. Lectures on phase transition and the renormalization group lectures on phase transition and the renormalization group, 1992. J. Phys. Soc. Japan 68, 3236–3243.
Horvath, A., Miskei, M., Ambrus, V., Vendruscolo, M., Fuxreiter, M., 2020. Sequence-based prediction of protein binding mode landscapes. PLoS Comput. Biol. 16, e1007864.
Huggins, M.L., 1941. Solutions of long chain compounds. J. Chem. Phys. 9, 440.
Hughes, M.P., Goldschmidt, L., Eisenberg, D.S., 2021. Prevalence and species distribution of the low-complexity, amyloid-like, reversible, kinked segment structural motif in amyloid-like fibrils. J. Biol. Chem. 297.
Hyman, A.A., Weber, C.A., Jülicher, F., 2014. Liquid-liquid phase separation in biology. Annu. Rev. Cell Dev. Biol. 30, 39–58.
Ikenoue, T., Lee, Y.-H., Kardos, J., Yagi, H., Ikegami, T., Naiki, H., Goto, Y., 2014. Heat of supersaturation-limited amyloid burst directly monitored by isothermal titration calorimetry. Proc. Natl. Acad. Sci. USA 111, 6654–6659.
Iserman, C., Roden, C.A., Boerneke, M.A., Sealfon, R.S.G., McLaughlin, G.A., Jungreis, I., Fritch, E.J., Hou, Y.J., Ekena, J., Weidmann, C.A., others, 2020. Genomic RNA elements drive phase separation of the SARS-CoV-2 nucleocapsid. Mol. Cell 80, 1078–1091.
Ishimoto, C., Tanaka, T., 1977. Critical behavior of a binary mixture of protein and salt water. Phys. Rev. Lett. 39, 474.
Jawerth, L., Fischer-Friedrich, E., Saha, Suropriya, Wang, J., Franzmann, T., Zhang, X., Sachweh, J., Ruer, M., Ijavi, M., Saha, Shambaditya, others, 2020. Protein condensates as aging Maxwell fluids. Science 370, 1317–1323.
Kamagata, K., 2021. Single-molecule microscopy meets molecular dynamics simulations for characterizing the molecular action of proteins on DNA and in liquid condensates. Front. Mol. Biosci. 1139.
Kamagata, K., Iwaki, N., Hazra, M.K., Kanbayashi, S., Banerjee, T., Chiba, R., Sakomoto, S., Gaudon, V., Castaing, B., Takahashi, H., others, 2021. Molecular principles of recruitment and dynamics of guest proteins in liquid droplets. Sci. Rep. 11, 1–13.
Kamagata, K., Kanbayashi, S., Honda, M., Itoh, Y., Takahashi, H., Kameda, T., Nagatsugi, F., Takahashi, S., 2020. Liquid-like droplet formation by tumor suppressor p53 induced by multivalent electrostatic interactions between two disordered domains. Sci. Rep. 10, 1–12.
Kang, J., Lim, L., Song, J., 2018. ATP enhances at low concentrations but dissolves at high concentrations liquid-liquid phase separation (LLPS) of ALS/FTD-causing FUS. Biochem. Biophys. Res. Commun. 504, 545–551.
Kar, M., Dar, F., Welsh, T.J., Vogel, L., Kühnemuth, R., Majumdar, A., Krainer, G., Franzmann, T.M., Alberti, S., Seidel, C.A.M., Knowles, T.P.J., Hyman, A.A., Pappu, R.V., 2022. Phase Separating RNA Binding Proteins Form Heterogeneous Distributions of Clusters in Subsaturated Solutions. https://doi.org/10.1101/2022.02.03.478969 bioRxiv.
Kardos, J., Yamamoto, K., Hasegawa, K., Naiki, H., Goto, Y., 2004. Direct measurement of the thermodynamic parameters of amyloid formation by isothermal titration calorimetry. J. Biol. Chem. 279, 55308–55314.
Kato, M., Han, T.W., Xie, S., Shi, K., Du, X., Wu, L.C., Mirzaei, H., Goldsmith, E.J., Longgood, J., Pei, J., others, 2012. Cell-free formation of RNA granules: low complexity sequence domains form dynamic fibers within hydrogels. Cell 149, 753–767.
Kato, M., Yang, Y.-S., Sutter, B.M., Wang, Y., McKnight, S.L., Tu, B.P., 2019. Redox state controls phase separation of the yeast ataxin-2 protein via reversible oxidation of its methionine-rich low-complexity domain. Cell 177, 711–721.
Keating, C.D., 2012. Aqueous phase separation as a possible route to compartmentalization of biological molecules. Acc. Chem. Res. 45, 2114–2124.
Keber, F.C., Nguyen, T., Brangwynne, C.P., Wühr, M., 2021. Evidence for widespread cytoplasmic structuring into mesoscopic condensates. bioRxiv. https://doi.org/10.1101/2021.12.17.473234.
Kelley, F.M., Favetta, B., Regy, R.M., Mittal, J., Schuster, B.S., 2021. Amphiphilic proteins coassemble into multiphasic condensates and act as biomolecular surfactants. Proc. Natl. Acad. Sci. USA 118 (51), e2109967118.
Kienzle, C., von Blume, J., 2014. Secretory cargo sorting at the trans-Golgi network. Trends Cell Biol. 24, 584–593.
Kiledjian, M., Dreyfuss, G., 1992. Primary structure and binding activity of the hnRNP U protein: binding RNA through RGG box. EMBO J. 11, 2655–2664.
Kim, T.H., Payliss, B.J., Nosella, M.L., Lee, I.T.W., Toyama, Y., Forman-Kay, J.D., Kay, L.E., 2021. Interaction hot spots for phase separation revealed by NMR studies of a CAPRIN1 condensed phase. Proc. Natl. Acad. Sci. USA 118.
King, O.D., Gitler, A.D., Shorter, J., 2012. The tip of the iceberg: RNA-binding proteins with prion-like domains in neurodegenerative disease. Brain Res. 1462, 61–80.
Klaips, C.L., Jayaraj, G.G., Hartl, F.U., 2018. Pathways of cellular proteostasis in aging and disease. J. Cell Biol. 217, 51–63.
Klein, I.A., Boija, A., Afeyan, L.K., Hawken, S.W., Fan, M., Dall'Agnese, A., Oksuz, O., Henninger, J.E., Shrinivas, K., Sabari, B.R., others, 2020. Partitioning of cancer therapeutics in nuclear condensates. Science 368, 1386–1392.
Knee, K.M., Mukerji, I., 2009. Real time monitoring of sickle cell hemoglobin fiber formation by UV resonance Raman spectroscopy. Biochemistry 48, 9903–9911.
Koopman, M.B., Ferrari, L., Rüdiger, S.G.D., 2022. How do protein aggregates escape quality control in neurodegeneration? Trends Neurosci. 45, 257–271.
Kuechler, E.R., Jacobson, M., Mayor, T., Gsponer, J., 2022. GraPES: the granule protein enrichment server for prediction of biological condensate constituents. Nucleic Acids Res. 50, W384–W391.
Kumar, R., Neuser, N., Tyedmers, J., 2017. Hitchhiking vesicular transport routes to the vacuole: amyloid recruitment to the Insoluble Protein Deposit (IPOD). Prion 11, 71–81.
Kundra, R., Ciryam, P., Morimoto, R.I., Dobson, C.M., Vendruscolo, M., 2017. Protein homeostasis of a metastable subproteome associated with Alzheimer's disease. Proc. Natl. Acad. Sci. USA 114, E5703–E5711.
Ladenstein, R., Fischer, M., Bacher, A., 2013. The lumazine synthase/riboflavin synthase complex: shapes and functions of a highly variable enzyme system. FEBS J. 280, 2537–2563.
Lafontaine, D.L.J., Riback, J.A., Bascetin, R., Brangwynne, C.P., 2021. The nucleolus as a multiphase liquid condensate. Nat. Rev. Mol. Cell Biol. 22, 165–182.
Lagier-Tourenne, C., Polymenidou, M., Cleveland, D.W., 2010. TDP-43 and FUS/TLS: emerging roles in RNA processing and neurodegeneration. Hum. Mol. Genet. 19, R46–R64.
Lancaster, A.K., Nutter-Upham, A., Lindquist, S., King, O.D., 2014. PLAAC: a web and command-line application to identify proteins with prion-like amino acid composition. Bioinformatics 30, 2501–2502.
Latham, A.P., Zhang, B., 2022. Unifying coarse-grained force fields for folded and disordered proteins. Curr. Opin. Struct. Biol. 72, 63–70.
Latonen, L., 2019. Phase-to-phase with nucleoli–stress responses, protein aggregation and novel roles of RNA. Front. Cell. Neurosci. 13, 151.
Lawrence, M.C., Colman, P.M., 1993. Shape complementarity at protein/protein interfaces. J. Mol. Biol. 234, 946–950.
Lee, M., Ghosh, U., Thurber, K.R., Kato, M., Tycko, R., 2020. Molecular structure and interactions within amyloid-like fibrils formed by a low-complexity protein sequence from FUS. Nat. Commun. 11, 1–14.
Lei, L., Wu, Z., Winklhofer, K.F., 2021. Protein quality control by the proteasome and autophagy: a regulatory role of ubiquitin and liquid-liquid phase separation. Matrix Biol. 100–101, 9–22.
Lemos, C., Schulze, L., Weiske, J., Meyer, H., Braeuer, N., Barak, N., Eberspächer, U., Werbeck, N., Stresemann, C., Lange, M., others, 2020. Identification of small molecules that modulate mutant p53 condensation. iScience 23, 101517.
Lerman, S., Zigman, S., Forbes, W.F., 1966. Properties of a cryoprotein in the ocular lens. Biochem. Biophys. Res. Commun. 22, 57–61.
Levine, A.J., 2019. Targeting therapies for the p53 protein in cancer treatments. Annu. Rev. Cell Biol. 3, 21–34.
Li, L., Srivastava, S., Andreev, M., Marciel, A.B., de Pablo, J.J., Tirrell, M.V., 2018. Phase behavior and salt partitioning in polyelectrolyte complex coacervates. Macromolecules 51, 2988–2995.
Li, P., Banjade, S., Cheng, H.-C., Kim, S., Chen, B., Guo, L., Llaguno, M., Hollingsworth, J.V., King, D.S., Banani, S.F., others, 2012. Phase transitions in the assembly of multivalent signalling proteins. Nature 483, 336–340.
Li, Y., Lubchenko, V., Vekilov, P.G., 2011. The use of dynamic light scattering and Brownian microscopy to characterize protein aggregation. Rev. Sci. Instrum. 82, 53106.
Li, Y., Lubchenko, V., Vorontsova, M.A., Filobelo, L., Vekilov, P.G., 2012. Ostwald-like ripening of the anomalous mesoscopic clusters in protein solutions. J. Phys. Chem. B 116, 10657–10664.
Liang, C., Hsieh, M.-C., Li, N.X., Lynn, D.G., 2018. Conformational evolution of polymorphic amyloid assemblies. Curr. Opin. Struct. Biol. 51, 135–140.
Lin, C.-W., Nocka, L.M., Stinger, B.L., DeGrandchamp, J.B., Lew, L.J.N., Alvarez, S., Phan, H.T., Kondo, Y., Kuriyan, J., Groves, J.T., 2022. A two-component protein condensate of the EGFR cytoplasmic tail and Grb2 regulates Ras activation by SOS at the membrane. Proc. Natl. Acad. Sci. USA 119, e2122531119.
Lin, Y., Mori, E., Kato, M., Xiang, S., Wu, L., Kwon, I., McKnight, S.L., 2016. Toxic PR poly-dipeptides encoded by the C9orf72 repeat expansion target LC domain polymers. Cell 167, 789–802.

Lopez, N., Camporeale, G., Salgueiro, M., Borkosky, S.S., Visentín, A., Peralta-Martinez, R., Loureiro, M.E., de Prat-Gay, G., 2021. Deconstructing virus condensation. PLoS Pathog. 17, e1009926.
Lyon, A.S., Peeples, W.B., Rosen, M.K., 2021. A framework for understanding the functions of biomolecular condensates across scales. Nat. Rev. Mol. Cell Biol. 22, 215–235.
Machyna, M., Heyn, P., Neugebauer, K.M., 2013. Cajal bodies: where form meets function. Wiley Interdiscip. Rev. RNA 4, 17–34.
Mackenzie, I.R., Nicholson, A.M., Sarkar, M., Messing, J., Purice, M.D., Pottier, C., Annu, K., Baker, M., Perkerson, R.B., Kurti, A., others, 2017. TIA1 mutations in amyotrophic lateral sclerosis and frontotemporal dementia promote phase separation and alter stress granule dynamics. Neuron 95, 808–816.
Maes, D., Vorontsova, M.A., Potenza, M.A.C., Sanvito, T., Sleutel, M., Giglio, M., Vekilov, P.G., 2015. Do protein crystals nucleate within dense liquid clusters? Acta Crystallogr. Sect. F Struct. Biol. Commun. 71, 815–822.
Maharana, S., Wang, J., Papadopoulos, D.K., Richter, D., Pozniakovsky, A., Poser, I., Bickle, M., Rizk, S., Guillén-Boixet, J., Franzmann, T.M., others, 2018. RNA buffers the phase separation behavior of prion-like RNA binding proteins. Science 360, 918–921.
Maji, S.K., Perrin, M.H., Sawaya, M.R., Jessberger, S., Vadodaria, K., Rissman, R.A., Singru, P.S., Nilsson, K.P.R., Simon, R., Schubert, D., others, 2009. Functional amyloids as natural storage of peptide hormones in pituitary secretory granules. Science 325, 328–332.
Malay, A.D., Suzuki, T., Katashima, T., Kono, N., Arakawa, K., Numata, K., 2020. Spider silk self-assembly via modular liquid-liquid phase separation and nanofibrillation. Sci. Adv. 6, eabb6030.
Manoharan, V.N., 2015. Colloidal matter: packing, geometry, and entropy. Science 349, 1253751.
Martin, E.W., Holehouse, A.S., Peran, I., Farag, M., Incicco, J.J., Bremer, A., Grace, C.R., Soranno, A., Pappu, R.V., Mittag, T., 2020. Valence and patterning of aromatic residues determine the phase behavior of prion-like domains. Science 367, 694–699.
Martin, E.W., Mittag, T., 2018. Relationship of sequence and phase separation in protein low-complexity regions. Biochemistry 57, 2478–2487.
Martin, E.W., Thomasen, F.E., Milkovic, N.M., Cuneo, M.J., Grace, C.R., Nourse, A., Lindorff-Larsen, K., Mittag, T., 2021. Interplay of folded domains and the disordered low-complexity domain in mediating hnRNPA1 phase separation. Nucleic Acids Res. 49, 2931–2945.
Mathieu, C., Pappu, R.V., Taylor, J.P., 2020. Beyond aggregation: pathological phase transitions in neurodegenerative disease. Science 370, 56–60.
Matthews, B.W., 1968. Solvent content of protein crystals. J. Mol. Biol. 33, 491–497.
McAlary, L., Chew, Y.L., Lum, J.S., Geraghty, N.J., Yerbury, J.J., Cashman, N.R., 2020. Amyotrophic lateral sclerosis: proteins, proteostasis, prions, and promises. Front. Cell. Neurosci. 14. https://doi.org/10.3389/fncel.2020.581907.
McCall, P.M., Kim, K., Fritsch, A.W., Iglesias-Artola, J.M., Jawerth, L.M., Wang, J., Ruer, M., Peychl, J., Poznyakovskiy, A., Guck, J., Alberti, S., Hyman, A.A., Brugués, J., 2020. Quantitative phase microscopy enables precise and efficient determination of biomolecular condensate composition. bioRxiv. https://doi.org/10.1101/2020.10.25.352823.
McManus, J.J., Charbonneau, P., Zaccarelli, E., Asherie, N., 2016. The physics of protein self-assembly. Curr. Opin. Colloid Interface Sci. 22, 73–79.
Mészáros, B., Erdos, G., Szabó, B., Schád, É., Tantos, Á., Abukhairan, R., Horváth, T., Murvai, N., Kovács, O.P., Kovács, M., others, 2020. PhaSePro: the database of proteins driving liquid-liquid phase separation. Nucleic Acids Res. 48, D360–D367.
Michael, J., Carroll, R., Swift, H.H., Steiner, D.F., 1987. Studies on the molecular organization of rat insulin secretory granules. J. Biol. Chem. 262, 16531–16535.
Milkovic, N.M., Mittag, T., 2020. Determination of protein phase diagrams by centrifugation. In: Intrinsically Disordered Proteins. Springer, pp. 685–702.
Milovanovic, D., Wu, Y., Bian, X., De Camilli, P., 2018. A liquid phase of synapsin and lipid vesicles. Science 361, 604–607.
Miskei, M., Horvath, A., Vendruscolo, M., Fuxreiter, M., 2020. Sequence-based prediction of fuzzy protein interactions. J. Mol. Biol. 432, 2289–2303.
Mittal, A., Holehouse, A.S., Cohan, M.C., Pappu, R.V., 2018. Sequence-to-conformation relationships of disordered regions tethered to folded domains of proteins. J. Mol. Biol. 430, 2403–2421.
Mohanty, P., Kapoor, U., Sundaravadivelu Devarajan, D., Phan, T.M., Rizuan, A., Mittal, J., 2022. Principles governing the phase separation of multidomain proteins. Biochemistry. https://doi.org/10.1021/acs.biochem.2c00210.
Molliex, A., Temirov, J., Lee, J., Coughlin, M., Kanagaraj, A.P., Kim, H.J., Mittag, T., Taylor, J.P., 2015. Phase separation by low complexity domains promotes stress granule assembly and drives pathological fibrillization. Cell 163, 123–133.
Monahan, Z., Ryan, V.H., Janke, A.M., Burke, K.A., Rhoads, S.N., Zerze, G.H., O'Meally, R., Dignon, G.L., Conicella, A.E., Zheng, W., others, 2017. Phosphorylation of the FUS low-complexity domain disrupts phase separation, aggregation, and toxicity. EMBO J. 36, 2951–2967.
Muiznieks, L.D., Sharpe, S., Pomès, R., Keeley, F.W., 2018. Role of liquid–liquid phase separation in assembly of elastin and other extracellular matrix proteins. J. Mol. Biol. 430, 4741–4753.
Mukherjee, A., Sudrik, C., Hu, Y., Arha, M., Stathos, M., Baek, J., Schaffer, D.V., Kane, R.S., 2020. CL6mN: rationally designed optogenetic photoswitches with tunable dissociation dynamics. ACS Synth. Biol. 9, 2274–2281.
Murakami, T., Qamar, S., Lin, J.Q., Schierle, G.S.K., Rees, E., Miyashita, A., Costa, A.R., Dodd, R.B., Chan, F.T.S., Michel, C.H., others, 2015. ALS/FTD mutation-induced phase transition of FUS liquid droplets and reversible hydrogels into irreversible hydrogels impairs RNP granule function. Neuron 88, 678–690.
Murray, D.T., Kato, M., Lin, Y., Thurber, K.R., Hung, I., McKnight, S.L., Tycko, R., 2017. Structure of FUS protein fibrils and its relevance to self-assembly and phase separation of low-complexity domains. Cell 171, 615–627.
Murthy, A.C., Dignon, G.L., Kan, Y., Zerze, G.H., Parekh, S.H., Mittal, J., Fawzi, N.L., 2019. Molecular interactions underlying liquid-liquid phase separation of the FUS low-complexity domain. Nat. Struct. Mol. Biol. 26, 637–648.
Muschol, M., Rosenberger, F., 1997. Liquid–liquid phase separation in supersaturated lysozyme solutions and associated precipitate formation/crystallization. J. Chem. Phys. 107, 1953–1962.
Nakashima, K.K., Vibhute, M.A., Spruijt, E., 2019. Biomolecular chemistry in liquid phase separated compartments. Front. Mol. Biosci. 6. https://doi.org/10.3389/fmolb.2019.00021.
Nassar, R., Dignon, G.L., Razban, R.M., Dill, K.A., 2021. The protein folding problem: the role of theory. J. Mol. Biol. 433, 167126.
Nesterov, S.V., Ilyinsky, N.S., Uversky, V.N., 2021. Liquid-liquid phase separation as a common organizing principle of intracellular space and biomembranes providing dynamic adaptive responses. Biochim. Biophys. Acta, Mol. Cell Res. 1868, 119102.
Nikfarjam, S., Ghorbani, M., Adhikari, S., Karlsson, A.J., Jouravleva, E.V., Woehl, T.J., Anisimov, M.A., 2019. Irreversible nature of mesoscopic aggregates in lysozyme solutions. Colloid J. 81, 546–554.
Ning, W., Guo, Y., Lin, S., Mei, B., Wu, Y., Jiang, P., Tan, X., Zhang, W., Chen, G., Peng, D., others, 2020. DrLLPS: a data resource of liquid–liquid phase separation in eukaryotes. Nucleic Acids Res. 48, D288–D295.
Nikolic, J., Le Bars, R., Lama, Z., Scrima, N., Lagaudrière-Gesbert, C., Gaudin, Y., Blondel, D., 2017. Negri bodies are viral factories with properties of liquid organelles. Nat. Commun. 8, 58.
Noji, M., Samejima, T., Yamaguchi, K., So, M., Yuzu, K., Chatani, E., Akazawa-Ogawa, Y., Hagihara, Y., Kawata, Y., Ikenaka, K., others, 2021. Breakdown of supersaturation barrier links protein folding to amyloid formation. Commun. Biol. 4, 1–10.
Nott, T.J., Petsalaki, E., Farber, P., Jervis, D., Fussner, E., Plochowietz, A., Craggs, T.D., Bazett-Jones, D.P., Pawson, T., Forman-Kay, J.D., others, 2015. Phase transition of a disordered nuage protein generates environmentally responsive membraneless organelles. Mol. Cell 57, 936–947.
Nusse, R., Clevers, H., 2017. Wnt β-catenin signaling, disease, and emerging therapeutic modalities. Cell 169, 985–999.
Oh, J., Yeom, S., Park, J., Lee, J.-S., 2022. The regional sequestration of heterochromatin structural proteins is critical to form and maintain silent chromatin. Epigenet. Chromatin 15, 1–13.
Orlando, G., Raimondi, D., Tabaro, F., Codicè, F., Moreau, Y., Vranken, W.F., 2019. Computational identification of prion-like RNA-binding proteins that form liquid phase-separated condensates. Bioinformatics 35, 4617–4623.
Orti, F., Navarro, A.M., Rabinovich, A., Wodak, S.J., Marino-Buslje, C., 2021. Insight into membraneless organelles and their associated proteins: drivers, Clients and Regulators. Comput. Struct. Biotechnol. J. 19, 3964–3977.
Overbeek, J.T.G., Voorn, M.J., 1957. Phase separation in polyelectrolyte solutions. Theory of complex coacervation. J. Cell. Comp. Physiol. 49, 7–26.
Pan, W., Galkin, O., Filobelo, L., Nagel, R.L., Vekilov, P.G., 2007. Metastable mesoscopic clusters in solutions of sickle-cell hemoglobin. Biophys. J. 92, 267–277.
Pan, W., Vekilov, P.G., Lubchenko, V., 2010. Origin of anomalous mesoscopic phases in protein solutions. J. Phys. Chem. B 114, 7620–7630.
Pancsa, R., Vranken, W., Mészáros, B., 2021. Computational resources for identifying and describing proteins driving liquid–liquid phase separation. Briefings Bioinf. 22. https://doi.org/10.1093/bib/bbaa408.
Parchure, A., Tian, M., Boyer, C.K., Bearrows, S.C., Rohli, K.E., Zhang, J., Ramazanov, B.R., Wang, Y., Stephens, S., von Blume, J., 2021. Liquid-liquid phase separation facilitates the biogenesis of secretory storage granules. bioRxiv. https://doi.org/10.1101/2021.12.22.472607.
Parmar, A.S., Muschol, M., 2009. Hydration and hydrodynamic interactions of lysozyme: effects of chaotropic versus kosmotropic ions. Biophys. J. 97, 590–598.
Parry, T.L., Melehani, J.H., Ranek, M.J., Willis, M.S., 2015. Functional amyloid signaling via the inflammasome, necrosome, and signalosome: new therapeutic targets in heart failure. Front. Cardiovasc. Med. 2, 25.
Patel, A., Lee, H.O., Jawerth, L., Maharana, S., Jahnel, M., Hein, M.Y., Stoynov, S., Mahamid, J., Saha, S., Franzmann, T.M., others, 2015. A liquid-to-solid phase transition of the ALS protein FUS accelerated by disease mutation. Cell 162, 1066–1077.
Pattanayak, G.K., Liao, Y., Wallace, E.W.J., Budnik, B., Drummond, D.A., Rust, M.J., 2020. Daily cycles of reversible protein condensation in cyanobacteria. Cell Rep. 32, 108032.
Pedley, A.M., Boylan, J.P., Chan, C.Y., Kennedy, E.L., Kyoung, M., Benkovic, S.J., 2022. Purine biosynthetic enzymes assemble into liquid-like condensates dependent on the activity of chaperone protein HSP90. J. Biol. Chem. 298.
Pedrote, M.M., Motta, M.F., Ferretti, G.D.S., Norberto, D.R., Spohr, T.C.L.S., Lima, F.R.S., Gratton, E., Silva, J.L., de Oliveira, G.A.P., 2020. Oncogenic gain of function in glioblastoma is linked to mutant p53 amyloid oligomers. iScience 23, 100820.
Peeples, W., Rosen, M.K., 2021. Mechanistic dissection of increased enzymatic rate in a phase-separated compartment. Nat. Chem. Biol. 17, 693–702.
Peran, I., Holehouse, A.S., Carrico, I.S., Pappu, R.V., Bilsel, O., Raleigh, D.P., 2019. Unfolded states under folding conditions accommodate sequence-specific conformational preferences with random coil-like dimensions. Proc. Natl. Acad. Sci. USA 116, 12301–12310.
Peran, I., Mittag, T., 2020. Molecular structure in biomolecular condensates. Curr. Opin. Struct. Biol. 60, 17–26.
Petronilho, E.C., Pedrote, M.M., Marques, M.A., Passos, Y.M., Mota, M.F., Jakobus, B., de Sousa, G., dos, S., da Costa, F.P., Felix, A.L., Ferretti, G.D.S., others, 2021. Phase

separation of p53 precedes aggregation and is affected by oncogenic mutations and ligands. Chem. Sci. 12, 7334–7349.
Petsev, D.N., Wu, X., Galkin, O., Vekilov, P.G., 2003. Thermodynamic functions of concentrated protein solutions from phase equilibria. J. Phys. Chem. B 107, 3921–3926.
Platten, F., Valadez-Pérez, N.E., Castañeda-Priego, R., Egelhaaf, S.U., 2015. Extended law of corresponding states for protein solutions. J. Chem. Phys. 142, 05B602_1.
Pombo, A., Dillon, N., 2015. Three-dimensional genome architecture: players and mechanisms. Nat. Rev. Mol. Cell Biol. 16, 245–257.
Posey, A.E., Ruff, K.M., Harmon, T.S., Crick, S.L., Li, A., Diamond, M.I., Pappu, R.V., 2018. Profilin reduces aggregation and phase separation of huntingtin N-terminal fragments by preferentially binding to soluble monomers and oligomers. J. Biol. Chem. 293, 3734–3746.
Poudyal, M., Patel, K., Sawner, A.S., Gadhe, L., Kadu, P., Datta, D., Mukherjee, S., Ray, S., Navalkar, A., Maiti, S., others, 2022. Liquid condensate is a common state of proteins and polypeptides at the regime of high intermolecular interactions. bioRxiv. https://doi.org/10.1101/2021.12.31.474648.
Privalov, P.L., 2007. Thermodynamic problems in structural molecular biology. Pure Appl. Chem. 79, 1445–1462.
Protter, D.S.W., Parker, R., 2016. Principles and properties of stress granules. Trends Cell Biol. 26, 668–679.
Qamar, S., Wang, G., Randle, S.J., Ruggeri, F.S., Varela, J.A., Lin, J.Q., Phillips, E.C., Miyashita, A., Williams, D., Ströhl, F., others, 2018. FUS phase separation is modulated by a molecular chaperone and methylation of arginine cation-π interactions. Cell 173, 720–734.
Rai, A.K., Chen, J.-X., Selbach, M., Pelkmans, L., 2018. Kinase-controlled phase transition of membraneless organelles in mitosis. Nature 559, 211–216.
Rao, B.S., Parker, R., 2017. Numerous interactions act redundantly to assemble a tunable size of P bodies in Saccharomyces cerevisiae. Proc. Natl. Acad. Sci. USA 114, E9569–E9578.
Ray, S., Chatterjee, D., Mukherjee, S., Patel, K., Mahato, J., Kadam, S., Krishnan, R., Sawner, A.S., Poudyal, M., Krishnamoorthy, G., Chowdhury, A., Padinhateeri, R., Maji, S.K., 2021. Spatiotemporal solidification of α-synuclein inside the liquid droplets. bioRxiv. https://doi.org/10.1101/2021.10.20.465113.
Reichheld, S.E., Muiznieks, L.D., Keeley, F.W., Sharpe, S., 2017. Direct observation of structure and dynamics during phase separation of an elastomeric protein. Proc. Natl. Acad. Sci. USA 114, E4408–E4415.
Riback, J.A., Katanski, C.D., Kear-Scott, J.L., Pilipenko, E.V., Rojek, A.E., Sosnick, T.R., Drummond, D.A., 2017. Stress-triggered phase separation is an adaptive, evolutionarily tuned response. Cell 168, 1028–1040.
Riback, J.A., Zhu, L., Ferrolino, M.C., Tolbert, M., Mitrea, D.M., Sanders, D.W., Wei, M.-T., Kriwacki, R.W., Brangwynne, C.P., 2020. Composition-dependent thermodynamics of intracellular phase separation. Nature 581, 209–214.
Roden, C., Gladfelter, A.S., 2021. RNA contributions to the form and function of biomolecular condensates. Nat. Rev. Mol. Cell Biol. 22, 183–195.
Rouaud, F., Sluysmans, S., Flinois, A., Shah, J., Vasileva, E., Citi, S., 2020. Scaffolding proteins of vertebrate apical junctions: structure, functions and biophysics. Biochim. Biophys. Acta, Biomembr. 1862, 183399.
Rubinstein, M., Colby, R.H., others, 2003. Polymer Physics. Oxford university press, New York.
Ruff, K.M., Dar, F., Pappu, R.V., 2021. Ligand effects on phase separation of multivalent macromolecules. Proc. Natl. Acad. Sci. USA 118.
Ruff, K.M., Roberts, S., Chilkoti, A., Pappu, R.V., 2018. Advances in understanding stimulus-responsive phase behavior of intrinsically disordered protein polymers. J. Mol. Biol. 430, 4619–4635.
Ryan, V.H., Dignon, G.L., Zerze, G.H., Chabata, C.V., Silva, R., Conicella, A.E., Amaya, J., Burke, K.A., Mittal, J., Fawzi, N.L., 2018. Mechanistic view of hnRNPA2 low-complexity domain structure, interactions, and phase separation altered by mutation and arginine methylation. Mol. Cell 69, 465–479.
Saar, K.L., Morgunov, A.S., Qi, R., Arter, W.E., Krainer, G., Lee, A.A., Knowles, T.P.J., 2021. Learning the molecular grammar of protein condensates from sequence determinants and embeddings. Proc. Natl. Acad. Sci. USA 118, e2019053118.
Safari, M.S., Byington, M.C., Conrad, J.C., Vekilov, P.G., 2017. Polymorphism of lysozyme condensates. J. Phys. Chem. B 121, 9091–9101.
Safari, M.S., Vorontsova, M.A., Poling-Skutvik, R., Vekilov, P.G., Conrad, J.C., 2015. Differential dynamic microscopy of weakly scattering and polydisperse protein-rich clusters. Phys. Rev. E 92, 42712.
Safari, M.S., Wang, Z., Tailor, K., Kolomeisky, A.B., Conrad, J.C., Vekilov, P.G., 2019. Anomalous dense liquid condensates host the nucleation of tumor suppressor p53 fibrils. iScience 12, 342–355.
Saha, S., Weber, C.A., Nousch, M., Adame-Arana, O., Hoege, C., Hein, M.Y., Osborne-Nishimura, E., Mahamid, J., Jahnel, M., Jawerth, L., others, 2016. Polar positioning of phase-separated liquid compartments in cells regulated by an mRNA competition mechanism. Cell 166, 1572–1584.
Sanders, D.W., Kedersha, N., Lee, D.S.W., Strom, A.R., Drake, V., Riback, J.A., Bracha, D., Eeftens, J.M., Iwanicki, A., Wang, A., others, 2020. Competing protein-RNA interaction networks control multiphase intracellular organization. Cell 181, 306–324.
Sawaya, M.R., Hughes, M.P., Rodriguez, J.A., Riek, R., Eisenberg, D.S., 2021. The expanding amyloid family: structure, stability, function, and pathogenesis. Cell 184, 4857–4873.
Sawyer, I.A., Sturgill, D., Dundr, M., 2019. Membraneless Nuclear Organelles and the Search for Phases within Phases, vol. 10. Wiley Interdiscip. Rev. RNA, e1514.
Schaefer, K.N., Peifer, M., 2019. Wnt/Beta-catenin signaling regulation and a role for biomolecular condensates. Dev. Cell 48, 429–444.
Schmidt, H., Putnam, A., Rasoloson, D., Seydoux, G., 2021. Protein-based condensation mechanisms drive the assembly of RNA-rich P granules. Elife 10, e63698.
Schmidt, H.B., Görlich, D., 2016. Transport selectivity of nuclear pores, phase separation, and membraneless organelles. Trends Biochem. Sci. 41, 46–61.
Schubert, R., Meyer, A., Baitan, D., Dierks, K., Perbandt, M., Betzel, C., 2017. Real-time observation of protein dense liquid cluster evolution during nucleation in protein crystallization. Cryst. Growth Des. 17, 954–958.
Schwayer, C., Shamipour, S., Pranjic-Ferscha, K., Schauer, A., Balda, M., Tada, M., Matter, K., Heisenberg, C.-P., 2019. Mechanosensation of tight junctions depends on ZO-1 phase separation and flow. Cell 179, 937–952.
Seviour, T., Wong, L.L., Lu, Y., Mugunthan, S., Yang, Q., Chanda Segaran, U., Bessarab, I., Liebl, D., Williams, R.B.H., Law, Y., others, 2020. Phase transitions by an abundant protein in the anammox extracellular matrix mediate cell-to-cell aggregation and biofilm formation. mBio 11 e02052–20.
Shapiro, D.M., Ney, M., Eghtesadi, S.A., Chilkoti, A., 2021. Protein phase separation arising from intrinsic disorder: first-principles to bespoke applications. J. Phys. Chem. B 125, 6740–6759.
Shin, Y., Brangwynne, C.P., 2017. Liquid phase condensation in cell physiology and disease. Science 357, eaaf4382.
Siezen, R.J., Fisch, M.R., Slingsby, C., Benedek, G.B., 1985. Opacification of gamma-crystallin solutions from calf lens in relation to cold cataract formation. Proc. Natl. Acad. Sci. USA 82, 1701–1705.
Simon, J.R., Carroll, N.J., Rubinstein, M., Chilkoti, A., López, G.P., 2017. Programming molecular self-assembly of intrinsically disordered proteins containing sequences of low complexity. Nat. Chem. 9, 509–515.
Sleutel, M., Van Driessche, A.E.S., 2014. Role of clusters in nonclassical nucleation and growth of protein crystals. Proc. Natl. Acad. Sci. USA 111, E546–E553.
Snead, W.T., Gladfelter, A.S., 2019. The control centers of biomolecular phase separation: how membrane surfaces, post-translational modifications, and active processes regulate condensation. Mol. Cell 76, 295.
So, M., Hall, D., Goto, Y., 2016. Revisiting supersaturation as a factor determining amyloid fibrillation. Curr. Opin. Struct. Biol. 36, 32–39.
Soranno, A., 2020. Physical basis of the disorder-order transition. Arch. Biochem. Biophys. 685, 108305.
Sosa, L., Torkko, J.M., Primo, M.E., Llovera, R.E., Toledo, P.L., Rios, A.S., Flecha, F.L.G., Trabucchi, A., Valdez, S.N., Poskus, E., Solimena, M., Ermácora, M.R., 2016. Biochemical, biophysical, and functional properties of ICA512/IA-2 RESP18 homology domain. Biochim. Biophys. Acta, Proteins Proteomics 1864, 511–522.
Spruijt, E., Westphal, A.H., Borst, J.W., Cohen Stuart, M.A., van der Gucht, J., 2010. Binodal compositions of polyelectrolyte complexes. Macromolecules 43, 6476–6484.
Su, X., Ditlev, J.A., Hui, E., Xing, W., Banjade, S., Okrut, J., King, D.S., Taunton, J., Rosen, M.K., Vale, R.D., 2016. Phase separation of signaling molecules promotes T cell receptor signal transduction. Science 352, 595–599.
Sun, Z., Diaz, Z., Fang, X., Hart, M.P., Chesi, A., Shorter, J., Gitler, A.D., 2011. Molecular determinants and genetic modifiers of aggregation and toxicity for the ALS disease protein FUS/TLS. PLoS Biol. 9, e1000614.
Taratuta, V.G., Holschbach, A., Thurston, G.M., Blankschtein, D., Benedek, G.B., 1990. Liquid-liquid phase separation of aqueous lysozyme solutions: effects of pH and salt identity. J. Phys. Chem. 94, 2140–2144.
Tesei, G., Schulze, T.K., Crehuet, R., Lindorff-Larsen, K., 2021. Accurate model of liquid–liquid phase behavior of intrinsically disordered proteins from optimization of single-chain properties. Proc. Natl. Acad. Sci. USA 118, e2111696118.
Thomson, J.A., Schurtenberger, P., Thurston, G.M., Benedek, G.B., 1987. Binary liquid phase separation and critical phenomena in a protein/water solution. Proc. Natl. Acad. Sci. USA 84, 7079–7083.
Tiwary, A.K., Zheng, Y., 2019. Protein phase separation in mitosis. Curr. Opin. Cell Biol. 60, 92–98.
Toledo, P.L., Torkko, J.M., Müller, A., Wegbrod, C., Sönmez, A., Solimena, M., Ermácora, M.R., 2019. ICA512 RESP18 homology domain is a protein-condensing factor and insulin fibrillation inhibitor. J. Biol. Chem. 294, 8564–8576.
Tompa, P., Fuxreiter, M., 2008. Fuzzy complexes: polymorphism and structural disorder in protein–protein interactions. Trends Biochem. Sci. 33, 2–8.
Torquato, S., 2018. Perspective: basic understanding of condensed phases of matter via packing models. J. Chem. Phys. 149, 20901.
Tunyasuvunakool, K., Adler, J., Wu, Z., Green, T., Zielinski, M., Zidek, A., Bridgland, A., Cowie, A., Meyer, C., Laydon, A., others, 2021. Highly accurate protein structure prediction for the human proteome. Nature 596, 590–596.
Turoverov, K.K., Kuznetsova, I.M., Fonin, A.V., Darling, A.L., Zaslavsky, B.Y., Uversky, V.N., 2019. Stochasticity of biological soft matter: emerging concepts in intrinsically disordered proteins and biological phase separation. Trends Biochem. Sci. 44, 716–728.
Updike, D.L., Hachey, S.J., Kreher, J., Strome, S., 2011. P granules extend the nuclear pore complex environment in the C. elegans germ line. J. Cell Biol. 192, 939–948.
Ura, T., Kagawa, A., Yagi, H., Tochio, N., Kigawa, T., Mikawa, T., Shiraki, K., 2020. Hyperactivation of L-lactate oxidase by liquid-liquid phase separation. bioRxiv. https://doi.org/10.1101/2020.12.08.416958.
Urosev, I., Lopez Morales, J., Nash, M.A., 2020. Phase separation of intrinsically disordered protein polymers mechanically stiffens fibrin clots. Adv. Funct. Mater. 30, 2005245.
Uversky, V.N., 2017. Protein intrinsic disorder-based liquid–liquid phase transitions in biological systems: complex coacervates and membrane-less organelles. Adv. Colloid Interface Sci. 239, 97–114.
Uversky, V.N., Dunker, A.K., 2010. Understanding protein non-folding. Biochim. Biophys. Acta, Proteins Proteomics 1804, 1231–1264.
Uversky, V.N., Finkelstein, A.V., 2019. Life in phases: intra-and inter-molecular phase transitions in protein solutions. Biomolecules 9, 842.

Van Der Lee, R., Buljan, M., Lang, B., Weatheritt, R.J., Daughdrill, G.W., Dunker, A.K., Fuxreiter, M., Gough, J., Gsponer, J., Jones, D.T., others, 2014. Classification of intrinsically disordered regions and proteins. Chem. Rev. 114, 6589–6631.
Vecchi, G., Sormanni, P., Mannini, B., Vandelli, A., Tartaglia, G.G., Dobson, C.M., Hartl, F.U., Vendruscolo, M., 2020. Proteome-wide observation of the phenomenon of life on the edge of solubility. Proc. Natl. Acad. Sci. USA 117, 1015–1020.
Vekilov, P.G., 2004. Dense liquid precursor for the nucleation of ordered solid phases from solution. Cryst. Growth Des. 4, 671–685.
Vernon, R.M., Chong, P.A., Tsang, B., Kim, T.H., Bah, A., Farber, P., Lin, H., Forman-Kay, J.D., 2018. Pi-Pi contacts are an overlooked protein feature relevant to phase separation. Elife 7, e31486.
Vernon, R.M., Forman-Kay, J.D., 2019. First-generation predictors of biological protein phase separation. Curr. Opin. Struct. Biol. 58, 88–96.
Vorontsova, M.A., Vekilov, P.G., Maes, D., 2016. Characterization of the diffusive dynamics of particles with time-dependent asymmetric microscopy intensity profiles. Soft Matter 12, 6926–6936.
Walker, A.A., Holland, C., Sutherland, T.D., 2015. More than one way to spin a crystallite: multiple trajectories through liquid crystallinity to solid silk. Proc. R. Soc. B Biol. Sci. 282, 20150259.
Walker, F.O., 2007. Huntington's disease. Lancet 369, 218–228.
Wang, H., Yan, X., Aigner, H., Bracher, A., Nguyen, N.D., Hee, W.Y., Long, B.M., Price, G.D., Hartl, F.U., Hayer-Hartl, M., 2019. Rubisco condensate formation by CcmM in β-carboxysome biogenesis. Nature 566, 131–135.
Wang, J., Choi, J.-M., Holehouse, A.S., Lee, H.O., Zhang, X., Jahnel, M., Maharana, S., Lemaitre, R., Pozniakovsky, A., Drechsel, D., others, 2018. A molecular grammar governing the driving forces for phase separation of prion-like RNA binding proteins. Cell 174, 688–699.
Wang, X., Zhou, X., Yan, Q., Liao, S., Tang, W., Xu, P., Gao, Y., Li, Q., Dou, Z., Yang, W., others, 2022. LLPSDB v2.0: an updated database of proteins undergoing liquid–liquid phase separation in vitro. Bioinformatics 38, 2010–2014.
Warzecha, M., Safari, M.S., Florence, A.J., Vekilov, P.G., 2017. Mesoscopic solute-rich clusters in olanzapine solutions. Cryst. Growth Des. 17, 6668–6676.
Wei, M.-T., Elbaum-Garfinkle, S., Holehouse, A.S., Chen, C.C.-H., Feric, M., Arnold, C.B., Priestley, R.D., Pappu, R.V., Brangwynne, C.P., 2017. Phase behaviour of disordered proteins underlying low density and high permeability of liquid organelles. Nat. Chem. 9, 1118–1125.
Wilkins, D.K., Grimshaw, S.B., Receveur, V., Dobson, C.M., Jones, J.A., Smith, L.J., 1999. Hydrodynamic radii of native and denatured proteins measured by pulse field gradient NMR techniques. Biochemistry 38, 16424–16431.
Wolf, M., Roosen-Runge, F., Zhang, F., Roth, R., Skoda, M.W.A., Jacobs, R.M.J., Sztucki, M., Schreiber, F., 2014. Effective interactions in protein–salt solutions approaching liquid–liquid phase separation. J. Mol. Liq. 200, 20–27.
Wong, L.E., Kim, T.H., Muhandiram, D.R., Forman-Kay, J.D., Kay, L.E., 2020. NMR experiments for studies of dilute and condensed protein phases: application to the phase-separating protein CAPRIN1. J. Am. Chem. Soc. 142, 2471–2489.
Woodruff, J.B., Hyman, A.A., Boke, E., 2018. Organization and function of non-dynamic biomolecular condensates. Trends Biochem. Sci. 43, 81–94.
Wu, X., Qiu, H., Zhang, M., 2022. Interactions between membraneless condensates and membranous organelles at the presynapse: a phase separation view of synaptic vesicle cycle. J. Mol. Biol. 167629.
Wunder, T., Cheng, S.L.H., Lai, S.-K., Li, H.-Y., Mueller-Cajar, O., 2018. The phase separation underlying the pyrenoid-based microalgal Rubisco supercharger. Nat. Commun. 9, 1–10.
Wunderlich, B., 1999. A classification of molecules, phases, and transitions as recognized by thermal analysis. Thermochim. Acta 340, 37–52.
Xu, S., Zhang, H., Qiao, B., Wang, Y., 2021. Review of liquid–liquid phase separation in crystallization: from fundamentals to application. Cryst. Growth Des. 21, 7306–7325.
Yadav, K., Yadav, A., Vashistha, P., Pandey, V.P., Dwivedi, U.N., 2019. Protein misfolding diseases and therapeutic approaches. Curr. Protein Pept. Sci. 20, 1226–1245.
Yanagisawa, H., Davis, E.C., 2010. Unraveling the mechanism of elastic fiber assembly: the roles of short fibulins. Int. J. Biochem. Cell Biol. 42, 1084–1093.
Yang, D.S., Saeedi, A., Davtyan, A., Fathi, M., Sherman, M.B., Safari, M.S., Klindziuk, A., Barton, M.C., Varadarajan, N., Kolomeisky, A.B., others, 2021. Mesoscopic protein-rich clusters host the nucleation of mutant p53 amyloid fibrils. Proc. Natl. Acad. Sci. USA 118.
Yang, P., Mathieu, C., Kolaitis, R.-M., Zhang, P., Messing, J., Yurtsever, U., Yang, Z., Wu, J., Li, Y., Pan, Q., others, 2020. G3BP1 is a tunable switch that triggers phase separation to assemble stress granules. Cell 181, 325–345.
Yang, Y., Fang, Z., Chen, X., Zhang, W., Xie, Y., Chen, Y., Liu, Z., Yuan, W., 2017. An overview of pickering emulsions: solid-particle materials, classification, morphology, and applications. Front. Pharmacol. 8, 287. https://doi.org/10.3389/fphar.2017.00287.
Yewdall, N.A., André, A.A.M., Lu, T., Spruijt, E., 2021. Coacervates as models of membraneless organelles. Curr. Opin. Colloid Interface Sci. 52, 101416.
Ying, Q., Chu, B., 1987. Overlap concentration of macromolecules in solution. Macromolecules 20, 362–366.
Yoshizawa, T., Nozawa, R.-S., Jia, T.Z., Saio, T., Mori, E., 2020. Biological phase separation: cell biology meets biophysics. Biophys. Rev. 12, 519–539.
You, K., Huang, Q., Yu, C., Shen, B., Sevilla, C., Shi, M., Hermjakob, H., Chen, Y., Li, T., 2020. PhaSepDB: a database of liquid-liquid phase separation related proteins. Nucleic Acids Res. 48, D354–D359.
Youn, J.-Y., Dyakov, B.J.A., Zhang, J., Knight, J.D.R., Vernon, R.M., Forman-Kay, J.D., Gingras, A.-C., 2019. Properties of stress granule and P-body proteomes. Mol. Cell 76, 286–294.
Yuan, C., Levin, A., Chen, W., Xing, R., Zou, Q., Herling, T.W., Challa, P.K., Knowles, T.P.J., Yan, X., 2019. Nucleation and growth of amino acid and peptide supramolecular polymers through liquid–liquid phase separation. Angew. Chem. 131, 18284–18291.
Zang, K., Wang, H., Hartl, F.U., Hayer-Hartl, M., 2021. Scaffolding protein CcmM directs multiprotein phase separation in β-carboxysome biogenesis. Nat. Struct. Mol. Biol. 28, 909–922.
Zhang, Y., Narlikar, G.J., Kutateladze, T.G., 2021. Enzymatic reactions inside biological condensates. J. Mol. Biol. 433, 166624.
Zhao, Y.G., Zhang, H., 2020. Phase separation in membrane biology: the interplay between membrane-bound organelles and membraneless condensates. Dev. Cell 55, 30–44.
Zhou, H.-X., Nguemaha, V., Mazarakos, K., Qin, S., 2018. Why do disordered and structured proteins behave differently in phase separation? Trends Biochem. Sci. 43, 499–516.
Zihni, C., Mills, C., Matter, K., Balda, M.S., 2016. Tight junctions: from simple barriers to multifunctional molecular gates. Nat. Rev. Mol. Cell Biol. 17, 564–580.